MID-AMERICA TRANSPORTATION CENTER

Report # MATC-MS&T: 130-1

Final Report
WBS:25-1121-0005-130-1

A Smart Assistance System for Increasing the Safety of Transportation Workers

Ruwen Qin, Ph.D.
Associate Professor
Department of Engineering Management & Systems Engineering
Missouri University of Science and Technology

Suzanna K. Long, Ph.D.
Professor

Mohammad Monjurul Karim, B.S.
Research Assitant

Pranav Godse, M.S.
Research Assistant

Md. Al-Amin, B.S.
Research Assitant

Katherine Linville, M.S.
Research Assistant

Jian Xue, B.S.
Student Intern

2018

A Cooperative Research Project sponsored by
U.S. Department of Transportation- Office of the Assistant Secretary for Research and Technology

A Smart Assistance System for Increasing the Safety of Transportation Workers

Ruwen Qin, Ph.D.
Associate Professor
Department of Engineering Management & Systems Engineering
Missouri University of Science and Technology

Mohammad Monjurul Karim, B.S.
Research Assistant
Department of Engineering Management & Systems Engineering
Missouri University of Science and Technology

Suzanna K. Long, Ph.D.
Professor
Department of Engineering Management & Systems Engineering
Missouri University of Science and Technology

Katherine Linville, M.S.
Research Assistant
Department of Engineering Management & Systems Engineering
Missouri University of Science and Technology

Pranav Godse, M.S.
Research Assistant
Department of Engineering Management & Systems Engineering
Missouri University of Science and Technology

Jian Xue, B.S.
Student Intern
Department of Engineering Management & Systems Engineering
Missouri University of Science and Technology

Md. Al-Amin, B.S.
Research Assistant
Department of Engineering Management & Systems Engineering
Missouri University of Science and Technology

A Report on Research Sponsored by

Mid-America Transportation Center

University of Nebraska–Lincoln

December 2018

TECHNICAL REPORT DOCUMENTATION PAGE

1. Report No. 25-1121-0005-130-1	**2. Government Accession No.**	**3. Recipient's Catalog No.**
4. Title and Subtitle A Smart Assistance System for Increasing the Safety of Transportation Workers		**5. Report Date** December 2018 **6. Performing Organization Code**
7. Author(s) Ruwen Qin https://orcid.org/0000-0003-2656-8705; Suzanna Long https://orcid.org/0000-0001-6589-5528; Pranav Godse; Md. Al-Amin; Mohammad Monjurul Karim; Katherine Linville; Jian Xue		**8. Performing Organization Report No.** 25-1121-0005-130-1
9. Performing Organization Name and Address Mid-America Transportation Center 2200 Vine St. PO Box 830851 Lincoln, NE 68583-0851		**10. Work Unit No.** **11. Contract or Grant No.** 69A3551747107
12. Sponsoring Agency Name and Address Missouri University of Science and Technology 1201 N State St. Rolla, MO 65409		**13. Type of Report and Period Covered** Final Report (August 2017 – December 2018) **14. Sponsoring Agency Code** MATC TRB RiP No. 91994-13
15. Supplementary Notes		

16. Abstract

This project aims to design and prototype a smart system for assisting transportation workers in operations. The system is architected as a cyber-physical system (CPS) to create the abilities to sense and monitor transportation workers in their workplace, assess and predict their risk exposure and awareness levels, and assist them in operations, in a near real-time manner. The project employs methods of system analytics to build the digital twin of the physical system - transportation workers operating in the workplace. The digital twin is able to process and analyze incident report data, and sensed data of workers and their workplace, to model, understand, and predict worker operations, as well as to evaluate risk exposure in the workplace. The project further uses sensing, communication, and feedback technologies to seamlessly integrate the digital twin with its physical system to allow for real-time interaction and collaboration between them. Results from the project confirms the effectiveness of the proposed approach to architecting, creating, and functioning the smart assistance system for transportation workers. The delivered prototype model has provided a foundation for improving and implementing the safety enhancement system.

17. Key Words Hazardous material; highway transportation; transportation workers; safety; cyber-physical system	**18. Distribution Statement** No restrictions.		
19. Security Classif. (of this report) Unclassified	**20. Security Classif. (of this page)** Unclassified	**21. No. of Pages** 67	**22. Price**

Form DOT F 1700.7 (8-72) Reproduction of completed page authorized

Table of Contents

List of Figures

List of Tables

List of Abbreviations

Bluetooth Low Energy (BLE)
Convolutional Neural Network (CNN)
Cyber Physical System (CPS)
Deep Convolutional Neural Networks (DCNN)
Electromyography (EMG)
False Negative (FN)
False Positive (FP)
Feature Pyramid Network (FPN)
Global Positioning System (GPS)
Hazardous Material Highway Transportation Incident (HMHI)
Inertial Measurement Unit (IMU)
Light Emitting Diode (LED)
Leave One Out (LOO)
Neural Network (NN)
Personal Protection Equipment (PPE)
Radio Frequency Identification (RFID)
Regional based Convolutional Neural Network (RCNN)
Solid State Drive (SSD)
Support Vector Machine (SVM)
Train-Test Split (TTS)
True Negative (TN)
True Positive (TP)

Disclaimer

The contents of this report reflect the views of the authors, who are responsible for the facts and the accuracy of the information presented herein. This document is disseminated in the interest of information exchange. The report is funded partially by a grant from the U.S. Department of Transportation's University Transportation Centers Program. However, the U.S. Government assumes no liability for the contents or use thereof.

Abstract

This project aims to design and prototype a smart system for assisting transportation workers in operations. The system is architected as a cyber-physical system (CPS) to create the abilities to sense and monitor transportation workers in their workplace, assess and predict their risk exposure and awareness levels, and assist them in operations, in a near real-time manner. The project employs methods of system analytics to build the digital twin of the physical system - transportation workers operating in the workplace. The digital twin is able to process and analyze incident report data, and sensed data of workers and their workplace, to model, understand, and predict worker operations, as well as to evaluate risk exposure in the workplace. The project further uses sensing, communication, and feedback technologies to seamlessly integrate the digital twin with its physical system to allow for real-time interaction and collaboration between them. Results from the project confirms the effectiveness of the proposed approach to architecting, creating, and functioning the smart assistance system for transportation workers. The delivered prototype model has provided a foundation for improving and implementing the safety enhancement system.

Chapter 1 Introduction

1.1 Problem Statement

Transportation workers have a higher chance than many workforces to be exposed to various risks in their workplace (Bureau of Transportation Statistics, 2016). Workers who operate vehicles to transport hazardous materials (hazmat) and those in work zones are representative examples (PHMSA-Incident Statistics, FHWA-Work Zone Management Program). Most hazmat incidents occur because of human error or package failure (Bureau of Transportation Statistics, 2016), and the economic, social, and environmental consequences of hazmat incidents are usually severe (Office of Hazardous Materials Safety, 2011; 2017). Each year over 20,000 workers are injured in road construction work zones and there are about 121 workplace fatalities accounting for 1.5%~3% of all workplace fatalities annually.

Protecting transportation workers from risks and improving their ability to operate safely in their workplace is important. For example, drivers transporting hazmat must receive initial and recurring trainings on general awareness and familiarization of hazmat, safety training on emergency response, and measurements to protect them from the exposure to hazmat (PHMSA-Hazardous Transportation Training Requirement).

Yet well-trained transportation workers may still make mistakes or be exposed to risks in their workplace. Human beings have bounded abilities in vision, cognition, making judgements, and simultaneously handling multiple tasks, particularly in complex, dynamic working environments or in response to suddenly occurring situations. Improving their ability to operate appropriately and safely in work conditions such as in transporting hazmat and at work zones through assisting them in vision, cognition, and making the right decisions, all in a near real-time manner, is in particular need considering the quick growth of such work conditions (USDO,

2015).

The rapid development of sensor technology, data processing capabilities, control theory, and systems science, has promoted the growth of cyber-physical systems (CPS) that integrate those capabilities to create smart connected systems facilitating various industries including transportation (Khaitan and McCalley, 2015). Yet not much work has been done to particularly build CPS for increasing the safety of the transportation workforce. This research aims to design and prototype a smart assistance CPS as a cost-effective solution for assisting transportation workers in vision and cognition of their exposure to risks in their workplace, as well as guiding them in taking actions to reduce operating errors and the exposure to risks, in a near real-time manner.

Our proposed research is highly relevant to the Mid-American Transportation Center (MATC) theme. The prototype of the smart assistance CPS to be delivered at the end of this project is a new cost-effective solution for increasing the ability of transportation workers to operate appropriately and safely in transporting hazmat, at work zones, and in other work conditions. The reduction of incidents at these places, particularly those with severe consequences, increases the safety of involved traveling public and general public. The system is designed to be smart (i.e., autonomous, independently managed and operated) and mobile, allowing for a convenient implementation by various agencies in a wide range of locations.

1.2 Research Approach

Figure 1.1 following describes the smart assistance CPS and our approach to developing the system. This CPS is designed to have the abilities to sense, analyze, monitor and assist transportation workers in real-time for increasing their ability to operate appropriately and safely in their workplace. In figure 1.1 the subsystem in blue color provides the sensing and monitoring

functions, the analytics function is provided by the three subsystems in red color, and the subsystem in green color provides the assistance function. It can be seen that the assistance CPS for hazardous material transportation workers is created through building and integrating these subsystems. In the following section we briefly summarize the research methods for developing the CPS.

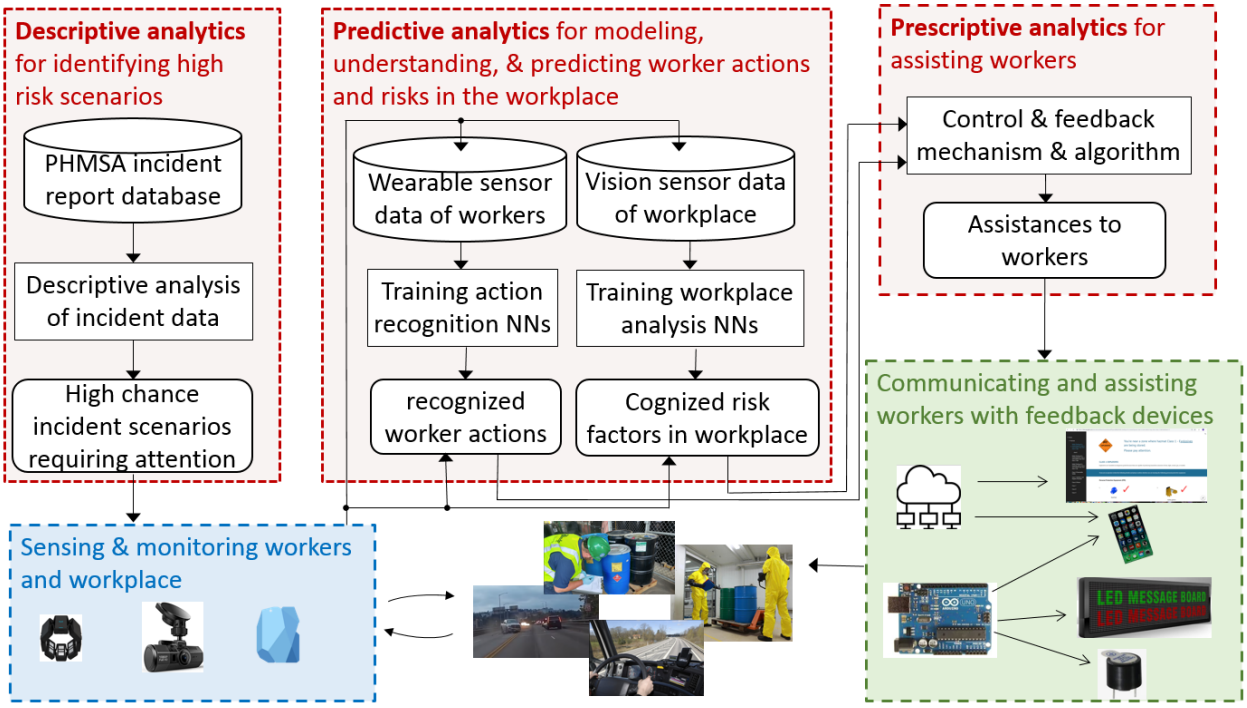

Figure 1.1 Schematic diagram of the smart CPS for assisting transportation workers in their workplace

1.3 Overview of the Research Methods

In this project we employ methods of system analytics to process and analyze sensed data of workers and their workplace to model, understand, and predict worker operations and behavior, as well as to evaluate risk exposure in the workplace. The project also explores communication and feedback devices to create the ability to deliver the assistance to

transportation workers in the workspace.

1.3.1 Descriptive Analysis of Incident Data

10 years hazardous material transportation incident data (2008-2017) are retrieved from the PHMSA incident reports database. Incident statistics shows that highway/road way transportation of hazardous materials has the largest numbers of fatalities, hospitalized injuries, and financial damages. Therefore, the incident data analysis of this project is focused on discovering characteristics of the incidents that caused fatalities, hospitalized injuries, or both. Based on the identified characteristics, a straightforward unfolding strategy is developed to identify high chance scenarios of hazardous material highway transportation incidents. Details of this descriptive analytic study are presented in Chapter 2. Outputs from the descriptive analysis help prioritize the efforts of sensing, monitoring, and assisting transportation workers.

1.3.2 Sensing and Predictive Sensor Data Analysis

To assist a transportation worker in operations, we need to know what the worker is doing or attempting to do, what risks the worker might be exposed to in the workspace, and what are the unique characteristics of the worker, to name a few. Sensing workers and their workplace to recognize worker activities and predict risks they may confront are important research components of this project. In this project we use wearable sensors to obtain inertial measurement unit (IMU) data of transportation workers during their operations. The data are used to train neural network (NN) models for classifying worker actions in operations and identifying abnormal worker actions and behavior. We use vision based sensors such as cameras to capture videos of the workplace. Then the data are used to fine-tune NN models offline. Obtained NN models can process real-time monitoring data to recognize worker actions in operations and identify risks that may occur. Details of this predictive analytic study are

presented in Chapter 3.

1.3.3 Prescriptive Analytics and Assistance Delivery

Timely and appropriately providing feedback to workers to enhance their awareness of risks, or providing operations guidance when needed, would reduce the chance of them being involved in, or causing, incidents. This project develops simple, reliable decision methods that mainly use thresholds to determine if any information needs to be delivered to transportation workers. Important efforts are made to examine and evaluate different options of communication (wired and wireless) and feedback devices (audio and visual). The design and prototyping of Feedback subsystem are discussed in detail in Chapter 4.

1.4 Organization of the Final Report

Following this introduction, Chapters 2-4 present major research efforts of this project, including research methods and findings. In Chapter 5 we conclude our studies and suggest future works. Literature cited in this report are listed in the References.

Chapter 2 Data Analysis for Identifying High Chance Scenarios of Hazardous Material Highway Transportation Incidents

2.1 Introduction

Hazardous Materials (HazMat) are those that can cause harm to living organisms, the environment, or property. They pose risks when being transported from one place to another. The transportation of hazardous materials needs to be operated in a safe manner by following safety procedures, such as The Hazardous Material Transportation Act (HMTA) enacted in 1975 (OSHA). In spite of following all the required safety procedures, incidents still occur during many transportation phases. An accident in which an affected person receives immediate medical treatment is called an incident. The persons affected include transportation workers, responders, and the general public. Incidents occurring in the transportation of hazardous materials may cause spillage, explosion, gas dispersion, fire, and environmental damages (ECFR 2018). Many of the incidents resulted in significant financial damages, injuries, and fatalities.

The Pipeline and Hazardous Material Safety Administration (PHMSA) is an agency of the United States Department of Transportation, which acquires and maintains the data and statistics of hazardous material incidents for all the modes of transportation including air, road or highway, rail, and water. The PHMSA statistics of hazardous material transportation incidents during 2008-2017 show that highway is the transportation mode with the largest numbers of fatalities, hospitalized injuries, and financial damages. Hazardous material highway incidents (HMHIs) account for over 95% of all fatalities, 72% of injuries, and 72% of all the damages, of all HazMat transportation incidents.

Protecting people from being hurt or killed by HMHIs is in high priority. Yet during the past ten years, there has been over 194 hospitalized injuries and 110 fatalities. Among them, over

85% were transportation workers, 12% were the general public, and the rest 3% were emergency responders. We are motivated to study these HMHIs that caused either fatalities or hospitalized injuries. Lowering the chance of these incidents can effectively reduce financial damages and the number of affected people.

Protecting or assisting workers in the transportation of hazardous materials would lower their vulnerability. This requires an investigation of the incident report data from the aspects of hazardous materials transported, incident causes, failure type, and so on. Relevant studies were found in the literature. Harwood et al. (1989) found the probability of hazmat release would be 13-15% given an incident involved in the transportation of hazardous materials. Moreover, 35-68% of the severe hazmat incidents were caused by traffic accidents. Abkowitz et al. (2001) discussed the economic impact of HMHIs for the year 1996. The work was able to give a cost scenario of the damages and suggest ways to mitigate the losses. Hwang et al. (2001) used the Chemical Accident Stochastic Risk Assessment Model (CASRAM) to estimate the statistical distribution of potential injuries and fatalities for each representative shipment developed in the commodity flow and shipment analysis. Clark and Besterfield-Sacre (2009) developed a decision model for mitigating hazmat release during the unloading phase using real data and an exploratory data modeling approach. This decision model identified the critical variables using an exploratory methodology involving latent class analysis (LCA), log linear modeling, and Bayesian Networking. Zhao et al. (2012) used Bayesian networks to prioritize the factors that influence hazmat transportation accidents. They compared 94 hazmat incidents to compute the posterior probability of each factor using an expectation-maximization learning algorithm. The findings and inference were used to take corrective actions and preventive measures to reduce the accidents. Yet a methodology is missing in the literature, which can be used to efficiently

review any sample of hazmat incidents, characterize the sample, and prioritize projects for incident reduction.

Therefore, this data analysis study has two objectives. Firstly, it will develop an efficient method for characterizing the uniqueness of the two samples of HMHIs: the incidents with hospitalized injuries (type-H HMHIs) and those with fatalities (type-F HMHIs). Following that, a straightforward method is developed for identifying high chance scenarios of type-H and type-F HMHIs. The remainder of the chapter is organized as follows. The next section delineates the methodology, followed by a section of results and discussions. We conclude the data analysis study at the end of this chapter to summarize management implications and outline the future work.

2.2 The Methodology of Incident Data Analysis

2.2.1 The Data

The data of HMHIs occurring during 2008-2017 were pulled from the PHMSA incident report database (PHMSA). This dataset is named type-A HMHIs in the paper. Then, two samples of the data, the type-H HMHIs and type-F HMHIs, were further extracted. The number of HMHIs during the ten-year period is 142,330, the number of HMHIs resulting in hospitalized injuries and fatalities are 167 and 91, respectively. The left plot of figure 2.1 shows that some of the HMHIs caused multiple hospitalized injuries and, therefore, the total number of hospitalized injuries is 194. Similarly, the right plot of figure 2.1 states that multiple fatalities were resulted in some HMHIs and the total number of fatalities is 110. The number of incidents that had either fatalities or hospitalized injuries is 246 because 12 incidents had both fatalities and hospitalized injuries.

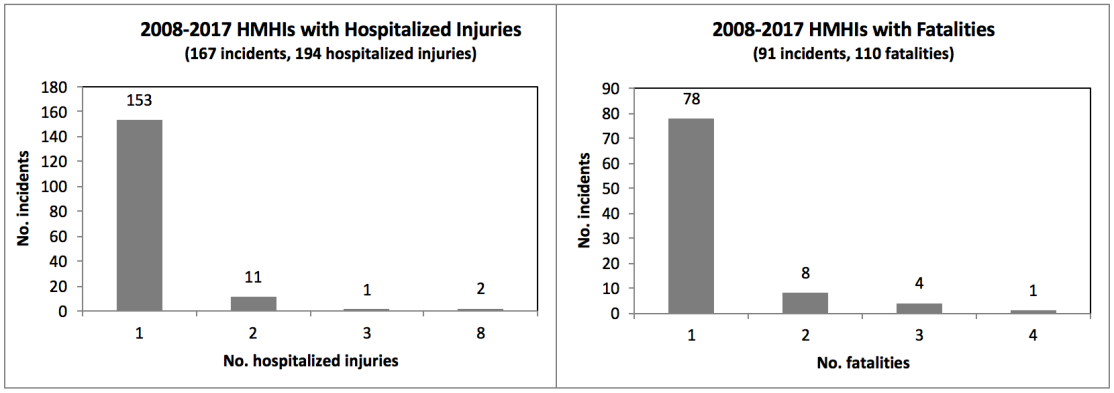

Figure 2.1 2008-2017 HMHIs with hospitalized injuries or fatalities

2.2.2 Data Fields

Fields of the HMHIs data cover all the information in the incident report Form 5800.1 (PHMSA). We particularly studied type-H and type-F incidents from the following lens (fields) to obtain a fundamental understanding of the incidents:

- Transportation phases: Let F_P denote the set of transportation phases, and F_P={in transit, in transit storage, loading, unloading}.
- HazMat classes: Let F_M denote the set of HazMat classes. There are 22 HazMat classes ranging from combustible liquid to very insensitive explosive. Some HMHIs did not report the material class, which are put in a category labeled as "blank".
- Incident causes: Let F_C denote the set of incident causes. There are 38 causes whose code ranging from 501 to 538. Some HMHIs did not release the cause, which are put in the category of "cause not reported".
- Incident results: Let F_R denote the set of incident results. F_R={environmental damage, explosion, fire, material entered waterway/sewer, spillage, vapor (gas) dispersion}.

These fields are all categorical data. Other fields can be considered as well, depending on the scope of the study.

2.2.3 Pareto-Type Distribution Charts

We created incident distribution charts for the two samples and their population, respectively, on each of the four fields selected. Figure 2.2 is an example that displays the distributions of type-F HMHIs and its population, respectively, on the 39 causes. The distribution charts we created are Pareto-type in that the categories of each field are arranged in the descending order of incident frequency. That is, let $n_{i(k),j}$ denote the number of type-j $(\in J = \{A, H, F\})$ HMHIs that takes the kth category of field i $(\in I = \{P, M, C, R\})$, then $n_{i(k),j} \geq n_{i(k'),j}$, $\forall k < k'$. Pareto-type distribution charts straightforwardly rank the categories of any field for each sample.

Various differences between type-F HMHIs and its population can be seen from the pairwise comparison in figure 2.2. Firstly, type-F HMHIs were caused by only ten causes, a subset of the 39 incident causes. Secondly, the ten causes relevant to type-F HMHIs do not fully overlap with the top ten causes for the population. Thirdly, although some of the 10 causes for type-F HMHIs has an overlap with a few of the top 10 causes for the population, they are not in the same ranked order in the two distribution charts. These differences indicate type-F HMHIs is not a homogenous sample of its population. We created a complete set of pairwise comparisons and each comparison is between one sample and its population (or the other sample) on one of the four fields. Therefore, there are twelve comparisons ($C_3^2 \times C_4^1 = 12$) in total including the one shown in figure 2.2.

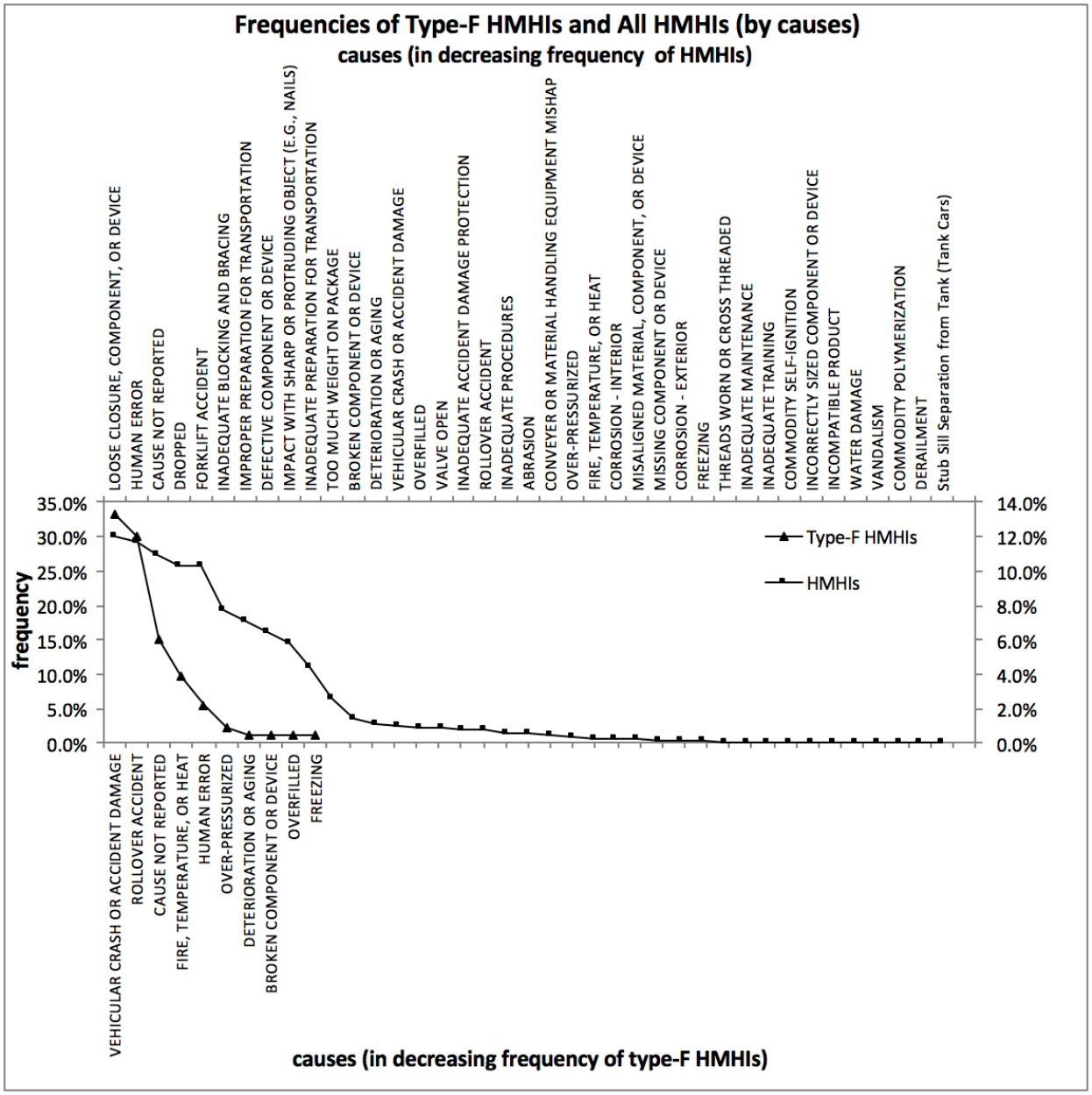

Figure 2.2 Pareto incident distribution charts of all HMHIs and HMHIs with fatalities

2.2.4 Indices for Measuring Heterogeneity

We further developed a set of indices for quantifying the heterogeneities observed in each of the twelve comparisons.

2.2.4.1 Overall Overlap

We define the overall overlap of two samples of HMHIs on a field to indicate the heterogeneity of their distribution supports on that field. Let $F_{i,j}$ ($\subseteq F_i$) be the distribution support of type-j ($\in J$) HMHIs on the field i ($\in I$). For example, $F_{P,H}$ contains transportation phases when type-H HMHIs occur. The overall overlap between any two samples of HMHIs, j and j', are

$$v_{i,(j,j')} = \frac{F_{i,j} \cap F_{i,j'}}{F_{i,j} \cup F_{i,j'}}. \tag{2.1}$$

$v_{i,(j,j')}$ takes a value within the segment $[0,1]$. The smaller the overall overlap, the greater the difference between their distribution support on the field i.

2.2.4.2 Intensive Overlap

We define intensive overlap to characterize the smallest subset of a distribution support where two samples of HMHIs largely overlap with each other. Let $F_{i(k),j}$ be the set containing the top k categories of field i for type-j HMHIs. In the comparison between type-j and j' HMHIs, k is an integer that can take a value from 1 to $\min\{K_{i,j}, K_{i,j'}\}$, where $K_{i,j}$ and $K_{i,j'}$ are the sizes of $F_{i,j}$ and $F_{i,j'}$, respectively. For example, $F_{C(3),F}$ contains the top three causes for type-F HMHIs. The overlap level of type- j and j' HMHIs that are distributed on their owned top k categories of field i is defined as:

$$o_{i(k),(j,j')} = \frac{F_{i(k),j} \cap F_{i(k),j'}}{2k - F_{i(k),j} \cap F_{i(k),j'}}, \tag{2.2}$$

which may vary as k is increasing. Let

$$o_{i,(j,j')} \equiv \max_{1 \le k \le \min\{K_{i,j}, K_{i,j'}\}} o_{i(k),(j,j')} \tag{2.3}$$

and let $K_{i,(j,j')}$ denote the (smallest) k at which $o_{i(k),(j,j')}$ is maximized. We may further normalize $K_{i,(j,j')}$ as the following so that the normalized index takes value from the segment [0, 1]:

$$\gamma_{i,(j,j')} = \frac{K_{i,(j,j')}}{\min\{K_{i,j}, K_{i,j'}\}}. \tag{2.4}$$

If $\gamma_{i,(j,j')}$ is small, approaching 0, then the intensive overlap, $o_{i,(j,j')}$, is significantly different than the overall overlap, $v_{i,(j,j')}$. Given $K_{i,(j,j')}$, we calculate the percentage of type-j HMHIs distributed on the top $K_{i,(j,j')}$ categories of field i:

$$\alpha_{i,(j,j')} = \frac{\sum_{k=1}^{K_{i,(j,j')}} n_{i(k),j}}{\sum_{k=1}^{K_{i,j}} n_{i(k),j}}, \tag{2.5}$$

The percentage for type-j', $\alpha_{i,(j',j)}$, is similarly calculated. A case with small values of $o_{i,(j,j')}$, $\alpha_{i,(j,j')}$ and $\alpha_{i,(j',j)}$ indicates a large difference between the two-types of HMHIs on the field i.

2.2.4.3 Distribution Distance

In a pairwise comparison between type-j and j' HMHIs, we measure the distance between their cumulative distribution functions (CDFs) at any (top) k categories of field i, and then we use the maximum distance to indicate the shape difference of incident distributions:

$$\beta_{i,(j,j')} = \max_{1 \le k \le \min\{K_{i,j}, K_{i,j'}\}} \left| \frac{\sum_{m=1}^{k} n_{i(m),j}}{\sum_{m=1}^{K_{i,j}} n_{i(m),j}} - \frac{\sum_{n=1}^{k} n_{i(n),j'}}{\sum_{n=1}^{K_{i,j'}} n_{i(n),j'}} \right|. \quad (2.6)$$

$\beta_{i,(j,j')}$ takes value from the segment [0, 1]. A large $\beta_{i,(j,j')}$ value indicates a difference between their distributions on the field i is identified.

2.2.4.4 Dashboard of the Indices

The indices indicating the heterogeneity of a sample of HMHIs on a field are summarized in figure 2.3.

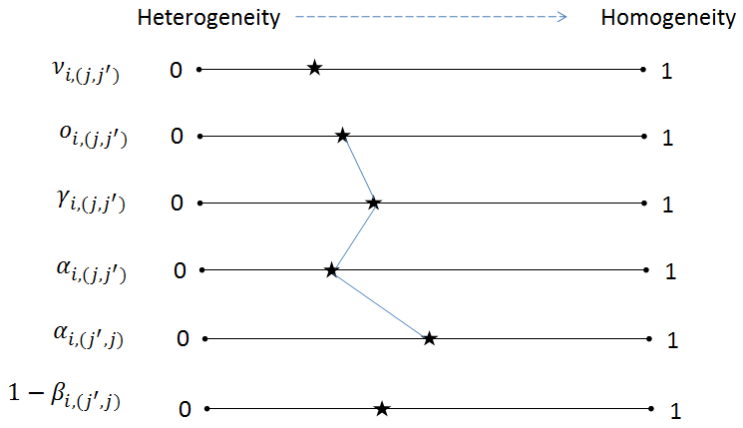

Figure 2.3 Dashboard of indices for evaluating the heterogeneity of an incident sample

2.2.4.5 An Unfolding Strategy for Identifying High Chance Scenarios of Incidents

Identifying scenarios with large chance of incidents are important because we can prioritize the efforts for incident prevention and risk mitigation. We characterize a scenario with a combination of the categorical values of selected variables such as transportation phase, hazmat class, and incident cause. Each combination is a cell, and we count the number of HMHIs in each cell. If there are a large number of cells and HMHIs were widely spread to many of them, it may

be difficult to identify high chance scenarios of incidents. The study developed an "unfolding strategy" to address this issue. For a sample of HMHIs, we first find a field where the HMHIs are intensively distributed on a small number of categories. We skip the categories with very low incident frequencies and may merge a few categories into one cell if we believe data in these categories share a certain similarity on at least one other field. One or more cells on the first field are created and we spread HMHIs into these cells. We further unfold each cell on the next selected field to form other cells by following a similar approach. We may unfold one cell at one time, and we may also unfold multiple cells at the same time. The Pivot Table function in Microsoft Excel can easily accommodate this unfolding strategy for identifying high chance scenarios of incidents.

2.3 Discussions of Incident Data Analysis Results

2.3.1 Pairwise Comparisons of Incident Samples for Identifying Sample Heterogeneity

In table 2.1 we performed the twelve pairwise comparisons listed below to verify the following assumptions.

Table 2.1 Pairwise comparisons of incident samples

(j, j')	(H, F)				(H, A)				(F, A)			
i	F	M	C	R	F	M	C	R	F	M	C	R
$K_{i,j}$	4	8	10	6	4	12	27	6	4	8	10	6
$K_{i,j'}$	4	12	27	6	4	23	39	7	4	23	39	7
$F_{i(k),j} \cap F_{i(k),j'}$	4	8	9	6	4	12	27	6	4	8	10	6
$v_{i,(j,j')}$	1.00	0.67	0.32	1.00	1.00	0.52	0.69	0.86	1.00	0.35	0.26	0.86
$o_{i,(j,j')}$	1.00	0.67	1.00	1.00	1.00	1.00	0.79	1.00	1.00	1.00	0.25	0.71
$\gamma_{i,(j,j')}$	0.50	0.22	0.13	0.71	0.25*	0.09	0.64	0.14	0.50	0.04	0.13	0.86
$\alpha_{i,(j,j')}$	0.75	0.90	0.64	0.97	0.48	0.82	0.99	0.95	0.77	0.52	0.55	1.00
$\alpha_{i,(j',j)}$	0.97	0.97	0.94	0.95	0.44	0.58	0.99	0.40	0.97	0.79	0.94	1.00
$\beta_{i,(j,j')}$	0.42	0.50	0.31	0.07	0.06	0.24	0.16	0.54	0.36	0.27	0.44	0.61

- Assumption 1: Type-H and type-F HMHIs are different

- Assumption 2: Type-H HMHIs differ than its population
- Assumption 3: Type-F HMHIs differ than its population

More importantly, if an assumption is found to be true, we further identify specific aspects on which the two samples are different.

2.3.1.1 Type-H vs. Type-F

The comparisons between type-H and type-F HMHIs indicate that they can be differentiated by incident causes, hazardous materials transported, and transportation phases, which are approximately in a decreasing order of the ability of differentiation.

- Type-H and type-F HMHIs can be clearly differentiated by incident causes. The overall overlap between them on the field of causes is only 32%, indicating at least one large group of causes is for one type but not the other. In this study, type-F HMHIs were caused by a smaller group of reasons (10) whereas type-H HMHIs were caused by a larger group (27). There are 18 causes that are reasons for type-H HMHIs, but not for type-F. The intensive overlap is 100%, very different from the overall overlap, which is based on only 13% of causes (4 out of 38 causes that exclude the "cause not reported"). 64% of type-H incidents and 94% of type-F incidents share the same top 4 causes: Vehicular crash or accident damage; rollover accident; fire, temperature, or heat; and human error. Yet the incident distribution of type-H on these causes is different than that of type-F, noticing that the maximum distance between their CDFs on this field is 31%, measured at their top 4 causes.
- Type-H and type-F incidents can be differentiated by the hazardous materials transported to a certain extent. Both the overall overlap and intensive overlap of them on the field of hazmat class are 67%, indicating that at least one group of materials is likely associated

with one type of incidents but not the other type. In our study, combustible liquid, oxidizer, poisonous gas and poisonous materials are associated with type-H HMHIs but not type-F. While the intensive overlap is also 67% (4 out of top 5 classes), it is based on just 22% of classes (5 out of 23), and it covers 90% of type-H incidents and 97% of type-F incidents. This indicates that the majority of type-H and type-F HMHIs are associated with a small group of materials and they are corrosive material, flammable combustible liquid, flammable gas, and nonflammable compressed gas. However, the distributions of the two types of incidents on these material classes are different, indicated by the 50% maximum distance of their CDFs on hazmat classes.

- A certain difference between Type-H and type-F HMHIs is identified from the perspective of transportation phases. Both the overall overlap and the intensive overlap of them on the field of phases are 100%, but this intensive overlap is based on 50% of phases (2 out of 4), and covers 75% of type-H incidents and 97% of type-F HMHIs. The majority (97%) of type-F HMHIs occurred during in-transit and unloading; the majority (95%) of type-H HMHIs occurred in unloading, in-transit, and loading. The maximum distance between their CDFs is 42%, which further confirms the distribution difference is present.
- Type-H and type-F incidents are similar in terms of incident results. Both the overall overlap and intensive overlap of them on the field of results are 100%. The intensive overlap includes 71% of result categories (5 out of 7 categories), 97% of type-H HMHIs and 95% of type-F HMHIs. This indicates the intensive overlap is similar to the overall overlap. The maximum distance between their CDFs is small, just 7%, indicating that distributions of these two samples on the field of results are also similar.

2.3.1.2 Type H vs. All HMHIs

Type-H differs from its population on the materials transported, incident causes, and results, which are approximately in a decreasing order of the ability of differentiation.

- Type-H HMHIs are associated with 12 hazmat classes, only 52% of the total classes. The distribution of type-H incidents on the 12 hazmat classes significantly differs from the population distribution, which is indicated by other indices.
- Type-H HMHIs are associated with 27 causes, about 69% of the total 39 causes. The intensive overlap is 79% (i.e., shared 22 out of 25 top causes), which is based on 99% of type-H HMHIs and 99% of all HMHIs. Therefore, the two overlaps are similar. However, the distribution of type-H HMHIs clearly differ from the population distribution.
- All results (exclude the category of "results not reported") happened to type-H HMHIs, but the distribution of type-H HMHIs is significantly different than the population distribution on results, indicated by other indices.

2.3.1.3 Type F vs. All HMHIs

Type-F differs from its population on incident causes, materials transported, results, and transportation phases that are approximately in a decreasing order of the ability of differentiation.

- Type-F HMHIs are associated with only 10 causes, about 26% of the total 39 causes. The intensive overlap of type-F with the population is 25% (their individual top 5 causes share 2 common causes). The distribution of type-F HMHIs on the 10 causes is significantly different from the population distribution.
- Type-F HMHIs are associated with only 8 hazmat classes, 35% of the total 23 classes. The number of type-F HMHIs is the largest when transporting flammable combustible liquid, about 79% of type-F HMHIs that occurred. Although this class of material is also

the top one class for its population, only 52% of them occurred when transporting it. The distribution of type-F incidents on the 8 hazmat classes is different than the population distribution.

- All results (excluding the category of "results not reported") happened to type-F incidents, but the distribution of type-F HMHIs is significantly different than the population distribution on results, indicated by other indices.
- Type-F HMHIs occurred in all of the four transportation phases, but its distribution on the four phases is very different than the population distribution, indicated by the maximum distance between their CDFs on the phases.

2.3.2 Identification of High Chance Scenarios of Incidents

Given the understanding of the HMHIs data attained from the pairwise comparisons, we were able to quickly identify high chance scenarios of incidents based on the unfolding strategy. Table 2.2 summarizes the top two scenarios in terms of the chance of type-H HMHIs.

Table 2.2 High Chance scenarios of type-H HMHIs

Scenarios	Phases	Hazmat Classes	Causes	Chance
1(H)	Loading Unloading	Corrosive material (class 8) Flammable combustible liquid (class 3) Flammable gas (class 2.1)	Human error (515) Defective component or device (508) Fire, temperature, or heat (512) Forklift accident (513) Deterioration or aging (510) Loose closure, component, or device (526) Over-pressurized (530) Dropped (511) Overfilled (529) Abrasion (501) Broken component or device (502)	72/167 (43.1%)
2(H)	In transit	Flammable combustible liquid (class 3)	Vehicular crash or accident damage (537) Rollover accident (531) Fire, temperature, or heat (512)	21/167 (12.6%)

For example, scenario 1(H) in table 2.2 is the one that type-H HMHIs (caused by 501, 502, 508, 510, 511, 512, 513, 515, 526, 529, or 530) often occur when loading or unloading classes 2.1, 3, or 8 hazardous materials. This scenario occurred at a probability of 43.1% based on the past ten-years HMHIs data.

Table 2.3 similarly summarizes the top two scenarios that concern type-F HMHIs.

Table 2.3 High chance scenarios of type-F HMHIs

Scenarios	Phases	Hazmat Classes	Causes	pct.
1(F)	In transit	Flammable combustible liquid (class 3)	Vehicular crash or accident damage (537) Rollover accident (531) Fire, temperature, or heat (512)	54/91 (59.3%)
2(F)	Loading Unloading	Flammable gas (class 2.1)	Human error (515) Deterioration or aging (510) Overfilled (529) Over-pressurized (530)	5/91 (5.5%)

From tables 2.2 and 2.3 it can be seen that scenarios 1(F) and 2(H) are the same scenario and 2(F) is a subset of 1(H). This finding suggests that we may merge the four scenarios into two scenarios, shown in table 2.4, and do not differentiate the assistances to transportation workers with respect to type-H and type-F HMHIs.

Table 2.4 High chance scenarios of HMHIs

Scenarios	Phases	Hazmat Classes	Causes	pct.
1(H/F)	Loading Unloading	Corrosive material (class 8) Flammable combustible liquid (class 3) Flammable gas (class 2.1)	Human error (515) Defective component or device (508) Fire, temperature, or heat (512) Forklift accident (513) Over-pressurized (530) Deterioration or aging (510) Loose closure, component, or device (526) Dropped (511) Overfilled (529) Abrasion (501) Broken component or device (502) Vehicular crash or accident damage (537)	77/246 (31.3%)
2(H/F)	In transit	Flammable combustible liquid (class 3)	Vehicular crash or accident damage (537) Rollover accident (531) Fire, temperature, or heat (512)	72/246 (29.3%)

2.4 Summary of Incident Data Analysis

This data analysis study collected 10-years (2008-2017) of data on incidents occurring in transporting hazardous materials on the highway (named HMHIs). Two specific samples of the data – HMHIs with fatalities (type-F HMHIs) and those with hospitalized injuries (type-H HMHIs) – were the focuses of this study. Then, a pairwise comparison based method was developed, which can be used to efficiently identify unique features of any incident sample, either against its population or in comparison with another sample. The method was implemented in analyzing the type-H and type-F HMHIs. Both samples were found to be non-homogenous samples of their population, and each of the two samples was found to have their own unique features. Based on the understanding of the two samples, the study developed a sequentially unfolding strategy that divides the space of incidents into subspaces and computes the frequency of incidents in the subspaces. Subspaces with a high frequency of incidents are of interest. Accordingly the paper presented six scenarios where assistances provided to

transportation workers can effectively lower the chance of type-H HMHIs, type-F HMHIs, or both of them.

Following this study, we have planned to implement the developed method in the analysis of large size samples (e.g., HMHIs caused by human error) and the prioritization of projects for transportation infrastructure improvement.

Chapter 3 Sensing and Predictive Sensor Data Analysis

This chapter presents two studies on processing and analyzing sensor data for safety enhancement. The first study aims to help workers better recognize objects or events that may cause risks in the workplace; the second study aims to recognize worker actions in operations to help intervene on risky behavior, prevent human error, and assist them when needed.

3.1 Computer Vision based Object Detection for Safety Enhancement

3.1.1 Background

Statistics shows that almost 68 percent of the world's population will live in urban areas by 2050 (UN, 2018). The urbanization is creating a huge pressure on the road transportation system. More people and vehicles are moving on roads every day. Their safety is one of the most important requirements for the road transportation system.

Meanwhile, growing vehicles and people are creating a huge amount of debris on the road which are causing car crashes. In the United States, about 50,695 crashes per year caused by road debris were reported in 2011-2014 (Tefft, 2016). Therefore, detecting objects on the road (including debris, pedestrians, vehicles, animals to name a few) and warning drivers ahead of time would help prevent crashes.

Deep learning has been playing an important role in object detection. This section presents a study that investigated the use of deep learning to process and analyze videos captured by a camera mounted on the vehicle to detect any sort of objects in various distances. The detection model can be integrated with a feedback device to warn the driver of possible obstacles on the road.

3.1.2 Related Work

In recent years, computer vision has been employed to help improve road transportation

safety. Tian et al. (2015) proposed a model which jointly optimizes pedestrian detection with semantic attributes. Their designed model has the ability to learn high-level features of objects from multiple data sources. Using video streams captured from surveillance cameras, Song et al. (2018) trained deep learning models for pedestrian and car detection, tracking, and action recognition. Xu et al. (2017) proposed a cross-modality learning framework for detecting pedestrians under adverse illumination conditions.

Work of Bojarski et al. (2016) was for supporting self-driving cars. Their convolutional neural network (CNN) model, trained on a dataset of less than one hundred hours of video, can operate a car avoiding obstacles. However, their trained network has some limitations. When a lane changes or a turn from one road to another is required, intervention of the human driver is necessary. Hane et al. (2015) followed a different approach to the obstacle detection, which extracts static obstacles from depth maps computed out of multiple consecutive images. This approach fuses obstacle detections over time and between cameras to estimate the free and occupied space around the vehicle.

Some other studies were focused on improving the computational speed. For example, Du et al. (2017) proposed a deep architecture that allows for parallel processing of multiple neural networks (NNs). A single shot deep CNN proposes pedestrian candidates and then multiple deep NNs are used in parallel for refining pedestrian candidates.

3.1.3 Object Detection for Safety Enhancement

A proposed safety enhancement system is illustrated in figure 3.1. It can use the car's own integrated sensors such as dashboard camera, radar, and rear cameras. The dashboard camera, mounted behind the windshield of the car, continuously captures high resolution images and feeds the image data to a deep learning algorithm of object detection. The algorithm

semantically detects individual objects coming in front of the car. Given the detection, the system proposes steering and brake commands that is compared with the driver's commands. The difference between them is measured. If the difference is higher than a pre-specified threshold value, the driver is notified with the measured difference and the proposed new command. The steering and brake commands to the vehicle may be automatically adjusted. Captured video data are stored in both a local Solid State Drive (SSD) and a cloud storage. Data stored in the cloud are used to tune the NN iteratively to improve the prediction quality. Our focus in this project is to train a deep learning algorithm for object detection.

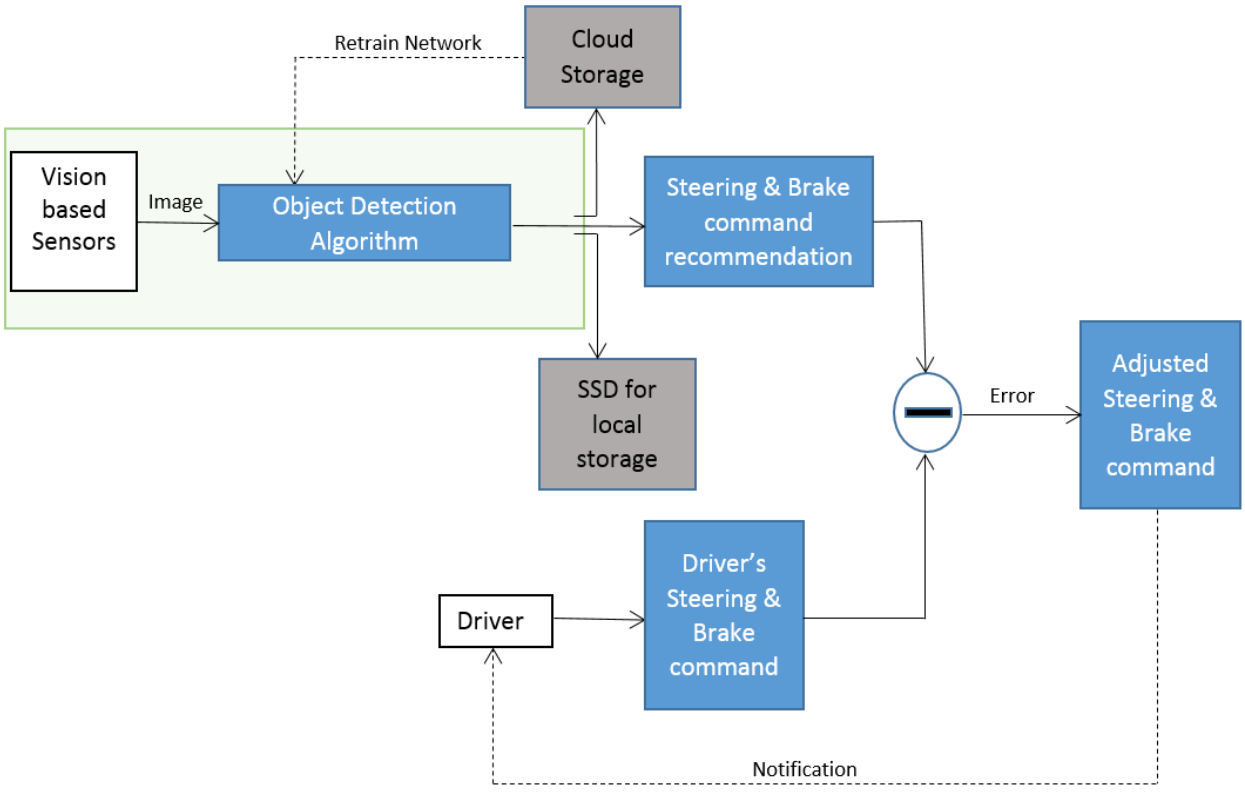

Figure 3.1 Schematic diagram of computer vision based smart driving system

Figure 3.2 shows the system architecture. The sensor module read out data from cameras, radar, Global Positioning System (GPS) and wheels, and then feeds the data to the detection module. The detection module uses a deep learning NN to segment and detect objects. The navigation module uses the GPS data to propose a location for the car and the corresponding path control. The vehicle module not only determines the steering angle and the brake control, but presents these data in a standard format that can be read by the user interface module. The user interface module displays the notification to the driver. All the data are stored in a local SSD device and uploaded to a cloud storage.

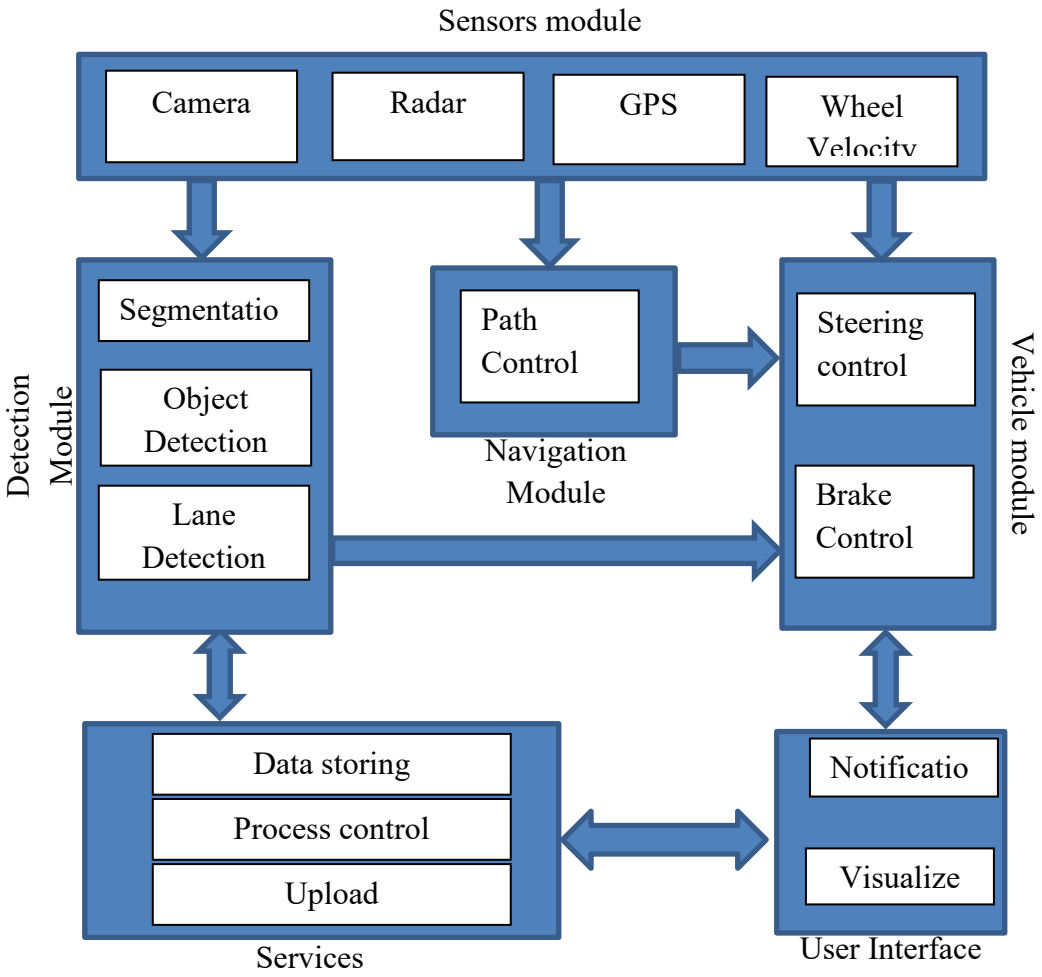

Figure 3.2 Schematic diagram of system architecture

3.1.4 A Deep Learning Algorithm for Object Detection

Regional based CNN (RCNN) has been shown to be effective in detecting and localizing objects in images. Mask RCNN (He et al., 2017) is one of these CNNs, which can perform region segmentation at the pixel level. In this project we chose the Mask RCNN algorithm for object detection and localization. Figure 3.3 illustrates the structure of Mask RCNN.

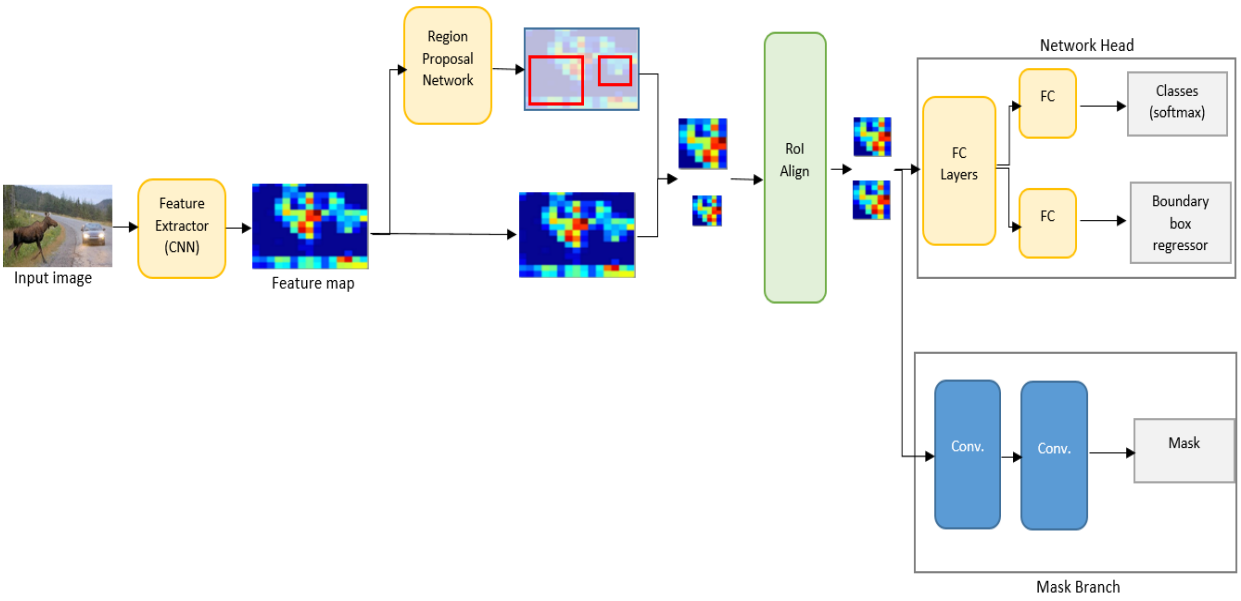

Figure 3.3 The structure of Mask RCNN

The backbone of the network is a CNN that works as a feature extractor. The architecture of this backbone network is a ResNet (He et al., 2016) based Feature Pyramid Network (FPN). This backbone CNN transforms the input image into feature maps. Then a region proposal network uses the feature maps to create region proposals. Each region proposal is extracted from the feature maps and converted into a fixed-size feature map. Then the RoIAlign operation aligns the extracted features with the input image to construct very accurate instance segmentation

masks. Following that, Mask RCNN adds a network head (fully convolutional layers) to produce the desired instance segmentations. This head branch has two subnetworks, one predicts object classes and the other predicts bounding boxes for each class. Besides the head branch, the network has an additional branch for predicting binary class masks for each class. The mask network branch predicts the mask independently from the network head predicting the class. For additional details, we refer interested readers to He et al. (2017).

3.1.5 An Example

3.1.5.1 The Training Dataset and the Mask RCNN

We adopted the Mask RCNN pre-trained on the Microsoft COCO dataset (Lin et al., 2014). The MS COCO dataset has more than 200,000 labeled images and it contains 1.5 million object instances in 80 categories including vehicles, humans, animals, and so on.

3.1.5.2 Testing Results

To test the pre-trained Mask RCNN, a testing dataset of 24,000 images was created by collecting videos from YouTube. In total 47 video clips with the framerate 30fps has been used to create this dataset. The average duration of each video clip is 17 seconds. The dataset contains images of traffic incidents captured by cameras mounted in the windshield of the vehicles. 2,850 images in the dataset were captured under bad weather driving conditions and 1,800 images were under low-light conditions. The resolution of the images are 1920 $\times$1080 pixels.

The pre-trained Mask RCNN successfully detected almost all cars and pedestrians in normal daylight driving conditions. Figure 3.4 shows some examples of detecting cars and pedestrians under a normal daylight condition driving conditions. Red masks in the figure indicate regions of predicted objects. False positive detections were observed, for example, the traffic lights in figure 3.4.

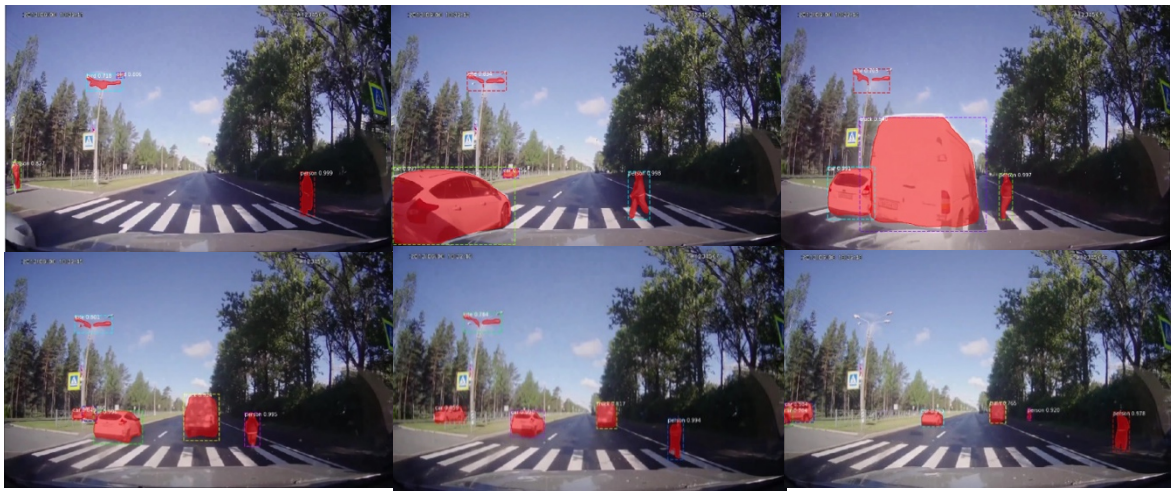

Figure 3.4 Detection results under a daytime driving condition

The Mask RCNN detector was also tested for bad weather driving conditions. It is able to recognize objects under such conditions but false detections were observed. Figure 3.5 illustrated the detection results under a bad weather condition. The leftmost image of the figure contains a false negative detection, where the detector couldn't detect a car. On the other hand, the detector mistakenly detected a region from the sky as a car in the rightmost image, which is a false positive detection. The middle image contains two vehicles and the detector detected both the vehicles.

Figure 3.5 Detection reults under a bad weather condition

Figure 3.6 further illustrates results of testing the Mask RCNN under a night driving condition. The leftmost image of the figure contains a false negative detection, where the detector couldn't detect a car. However, the following two frames contain positive detection. All the objects are detected in both of these frames.

Figure 3.6 Detection results under a nighttime driving condition

Besides vehicles, the Mask RCNN is also capable of detecting animals on the road, as figure 3.7 illustrates.

Figure 3.7 Animal detection

3.1.5.3 Detection Quality Assessment

The detection of an object in an image is represented as a bounding box. The bounding box contains both the object and some portion of the background, making it difficult to

determine if the detection is positive or negative. This issue is addressed by calculating the Intersection over Union (IoU) metric:

$$IoU = \frac{\text{Area of Overlap}}{\text{Area of Union}} \tag{3.1}$$

In the numerator the area of overlap between the prediction bounding box and the ground-truth bounding box is computed. And in the denominator the area encompassed by both boxes is computed.

To evaluate the detection quality of the Mask RCNN, an overlapping grid of ground truth objects and their predictions were calculated for the various driving conditions that the project has tested. In each overlapping grid, ground truth classes are listed on the horizontal axis; on the vertical axis the predicted classes are listed in the decreasing order of detection probability (i.e., the number in the bracket after each detected object). The grid describes the overlapping degree of the predicted objects with their respective ground truth. A 0.5 IoU threshold was used in the evaluation. That is, a prediction is correct if the IoU value of it is greater than 0.5.

Figure 3.8 (a) shows an image with detected objects under a normal daylight driving condition and figure 3.8 (b) displays the corresponding overlapping grid. In this test, all objects are detected correctly, with an IoU value greater than the detection threshold.

When testing the Mask RCNN for bad weather driving conditions, misclassified detections were observed. Figure 3.9 (a) shows the detection result under a bad weather condition and figure 3.9 (b) gives the corresponding overlapping grid. From the grid box it is observed that a car was misclassified as a truck and the model also failed to detect a car.

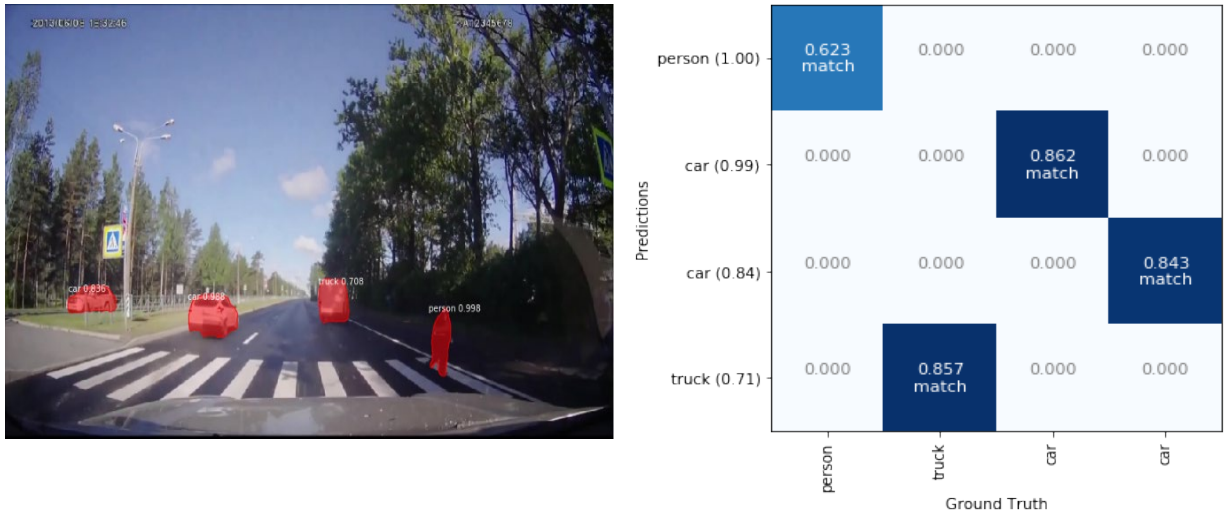

(a) (b)

Figure 3.8 Detection result in a daylight driving condition (a), the overlapping grid (b)

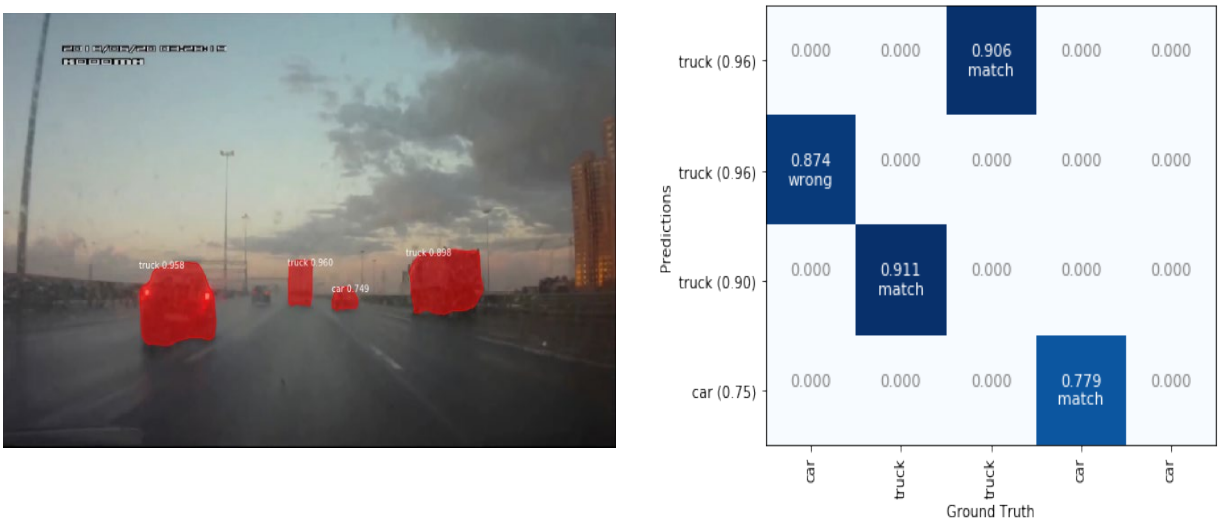

(a) (b)

Figure 3.9 Detection result under a bad weather condition (a), the overlapping grid (b)

The Mask RCNN can recognize objects on the road at night. Figure 3.10 (a) illustrates the detection result under a nighttime driving condition. The corresponding overlapping grid in figure 3.10 (b) further shows that multiple cars were not detected.

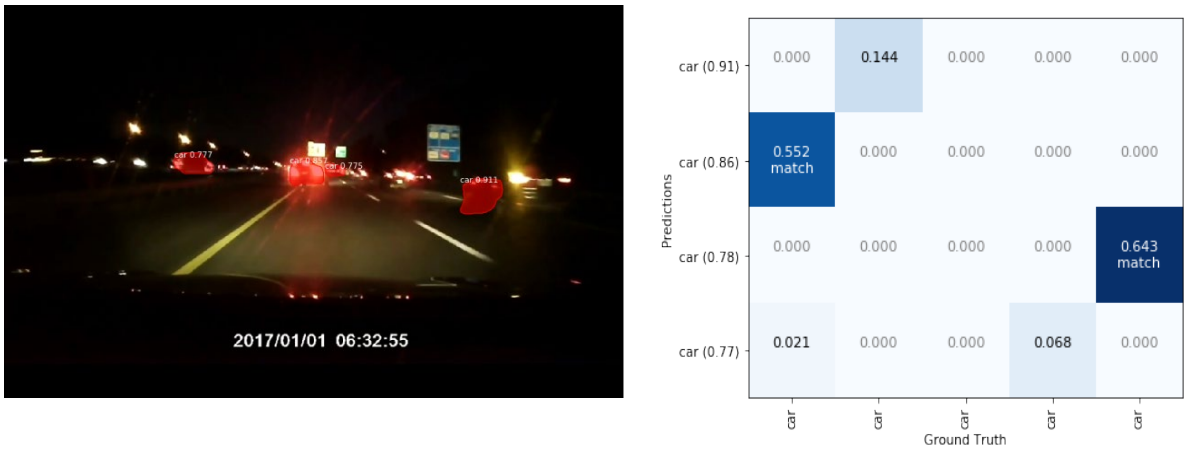

Figure 3.10 Detection result under a nighttime driving condition (a), the overlapping grid (b)

3.1.6 Conclusion

This section presented the use of Mask RCNN, a deep learning algorithm, for the detection and segmentation of objects from road scene videos. The Mask RCNN has been pre-trained on a large dataset containing 1.5 million images. The trained Mask RCNN was evaluated through testing it under multiple driving conditions. Detection results were in good quality under daylight driving conditions. False detections were observed when testing the model in bad weather and nighttime driving conditions. Improvement of the detection quality, particularly in low visibility conditions, would be required in order to provide reliable prediction results for assisting drivers in making decisions.

3.2 Worker Action Recognition using Wearable Sensors

3.2.1 Background

Safety has always been an important requirement for the transportation system (Raso et al., 2018). How transportation workers operate in their work have a huge impact on the safety of themselves and other people in the system. To be able to recognize and predict actions of

transportation workers in any phases of transportation would help prevent risky operations and human errors, thus reducing injuries, fatalities, and financial damage.

Relevant data of workers are needed to comprehend their actions in their workplace. Recent advancement in sensing technology has attracted the attention of researchers and practitioners. Sensors have been broadly used in many areas including manufacturing, healthcare, and transportation to name a few. We can deploy a suit of sensors in the workplace to collect meaningful data of workers and their interaction with the workplace. Different sensors such as vision based sensors, wearable sensors, and radio frequency identification (RFID) based sensors have their own merits and limitations. Vision based sensors, as Section 3.1 has discussed, have relatively high computing and storage requirements in data processing and modeling. RFID based sensors requires large infrastructure (Lara et al., 2013). Wearable sensors can be easily deployed to collect data of workers in operations (Nath et al., 2017). This section presents a study of using wearable sensors to capture, analyze, and model transportation worker actions in operations. Workers, wearable sensors, and machine learning methods are integrated to create the ability to recognize and predict worker actions. The output can be entered to the feedback system to generate assistance or prevention commends for workers.

3.2.2 Related Work

In recent years human activity recognition has become an important research topic. Many studies have presented remarkable results of activity recognition using wearable sensors data. Zhang and Sawchuk (2013) presented a human activity recognition framework that is based on wearable inertial sensors, compressed sensing, and sparse representation theory. Anguita et al. (2012) developed a multiclass classifier using Support Vector Machine (SVM). Catal et al. (2015) proposed a model of activity recognition which combines J48, logistic regression, and

multi-layer perceptron algorithms. A comprehensive study of wearable sensor based human activity recognition is in Shoaib et al. (2015), which delineated the usefulness of gyroscope with an accelerometer for classifying activities.

Yet, very limited work has been done which uses deep learning in activity recognition. Jiang and Yin (2015) assembled signal sequences of accelerometers and gyroscopes as activity images and, accordingly, employed Deep Convolutional Neural Networks (DCNN) to automatically learn optimal features from the activity images. Ha & Choi (2016) presented an approach to human activity recognition using CNN wherein they employed both the partial weight sharing and full weight sharing for the CNN models. Zeng et al. (2014) also proposed a CNN model which can automatically extract discriminative features of activities. They also applied the partial weight sharing technique to the processing of accelerometer signals. Nweke et al. (2018) provided an in-depth summary of deep learning methods for processing mobile and wearable sensors for human activity recognition.

3.2.3 Action Recognition using Deep Learning

Even though conventional pattern recognition has made tremendous progresses towards human activity recognition, it has several drawbacks:

1. The selection of features to extract is heuristic and heavily relies on human experience and domain knowledge. The specific knowledge can help in certain tasks but not for more general tasks.
2. Extracted features are shallow. This can only be used to recognize low level activities like walking and running, but not context-aware activities.
3. It requires a large amount of labeled trained data. Therefore, the method is undermined in unsupervised learning.

Deep learning is able to overcome those limitations. Figure 3.11 highlights the difference between conventional and deep learning approach.

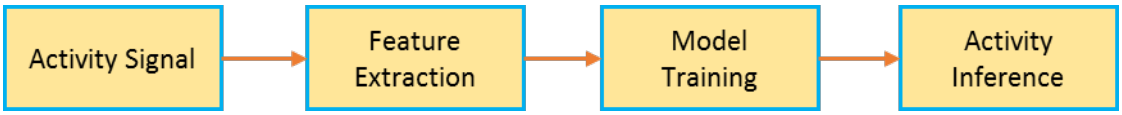

(a): Conventional approach

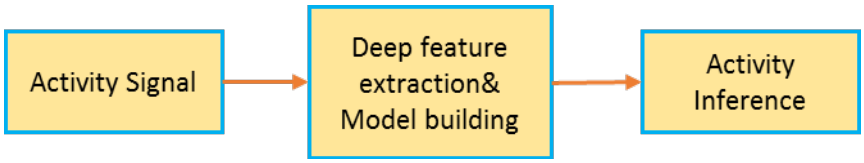

(b): Deep learning approach

Figure 3.11 Conventional vs deep learning methods in activity recognition

3.2.4 Data Preparation

3.2.4.1 Data Collection

To establish our logistic activity dataset, five actions commonly performed in logistic operations are chosen, namely: waiting, loading into trolley, pushing trolley, carrying load, and unloading from trolley. Table 3.1 lists these activities and a glimpse of them are shown in figure 3.12.

Table 3.1: List of tasks for logistic operation

Serial No.	Task name
1	Waiting
2	Loading into trolley
3	Pushing trolley
4	Carrying load
5	Unloading from trolley

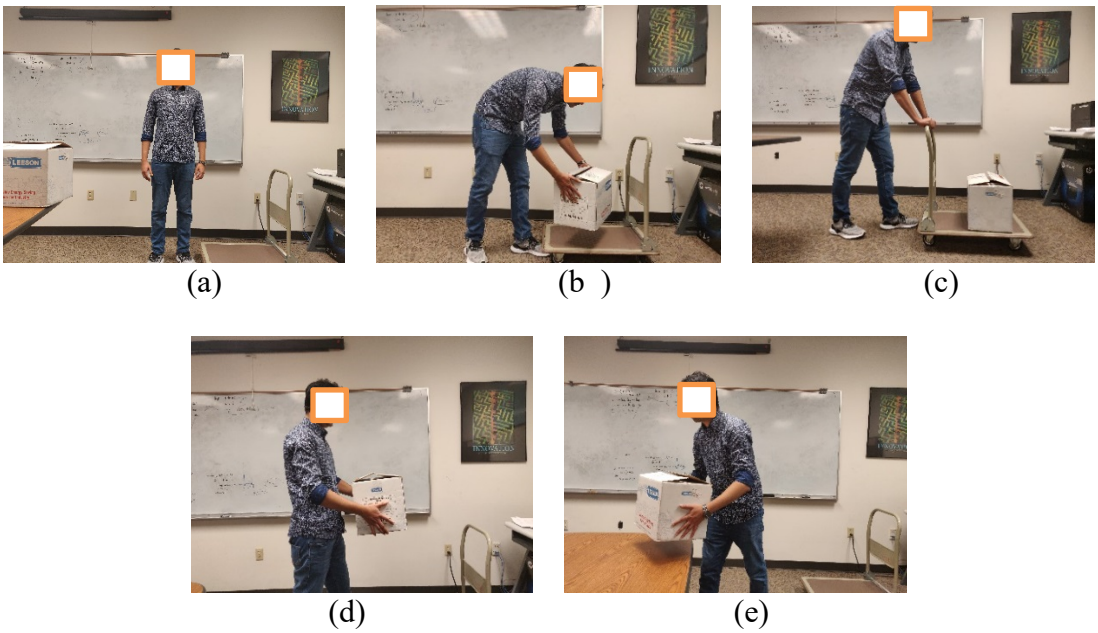

Figure 3.12 Common five logistic actions: (a) waiting, (b) loading the load to trolley, (c) pushing the trolley, (d) carrying the load, (e) unloading the load

Four subjects were invited to perform the five actions listed in table 3.1. A Myo armband, shown in figure 3.13, is embedded with IMU and EMG sensors. Two armbands were used in this study to collect data of participating subjects, with one armband worn on the left hand and the other on the right hand of each worker. One computer can collect data only from one armband at a time. Therefore two computers are used to collect data from two armbands. The IMU of the armband returns four types of signals (four channels of accelerations, three channels of angular velocities, four channels of orientations, and three channels of orientation Euler) at a sample rate of 50Hz. All channels of data were transmitted to receiving computers via a Bluetooth device.

Figure 3.13 Myo armband

3.2.4.2 Data Pre-Processing

The duration of each activity ranges from 2 to 6 seconds, not at a fixed length. Fixed length inputs are required to feed the data into a NN. Therefore, the collected IMU signals were converted into fixed length activity images with some preprocessing. The 13 channels of IMU signals are aligned horizontally, as figure 3.14 shows.

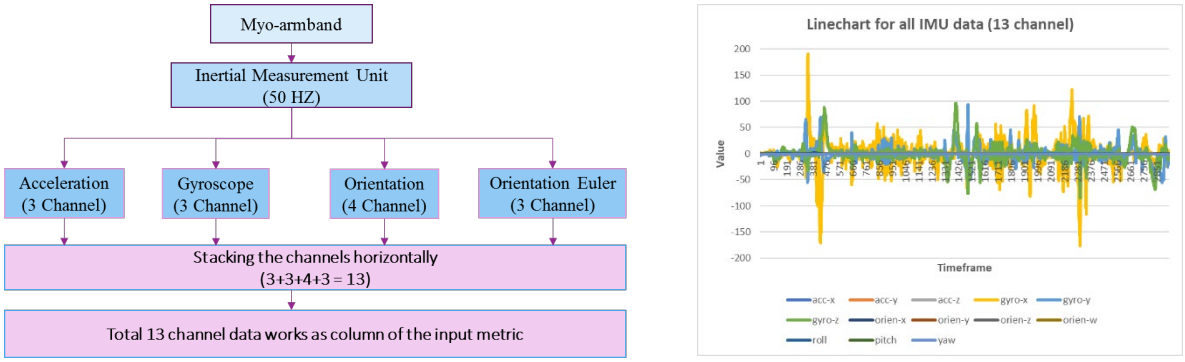

(a) (b)

Figure 3.14 Horizontally stacking the raw IMU signals (a), stacked IMU signals (b)

Each activity image is a 100 rows by 13 columns matrix that contains 2 seconds of IMU time series data, as figure 3.15 demonstrates. Figure 3.16 shows the method of generating activity images from raw IMU sensor data. Activity images were created by moving a sliding

window of size 100 rows by 13 columns along the row direction at a step size of 50 rows. An activity image was extracted from the IMU time series data at each stop. Therefore, two successive activity images have a 50% overlap.

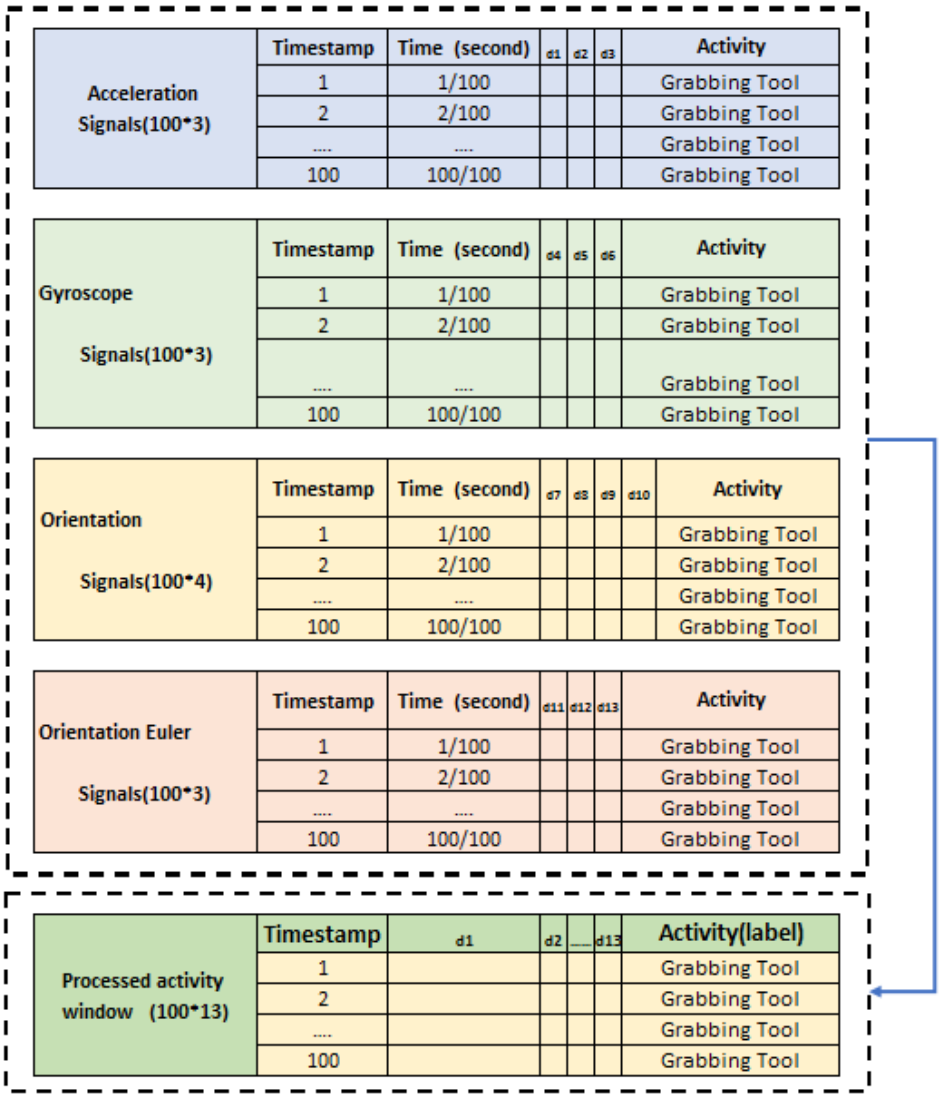

Figure 3.15 Preparing activity image from raw IMU signal

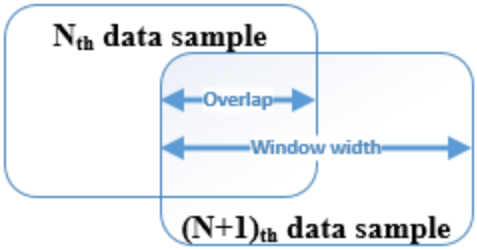

Figure 3.16 Window width and overlap ratio of activity windows

The worker activity dataset we created for this project contains five actions performed by five subjects. Each subject performed all of the five actions ten times. Therefore the activity dataset contains 200 samples of actions in total. However, some subjects were faster in their operations whereas others were comparatively slower. Therefore, the time taken to complete the activities varied subject to subject. Consequently, the number of activity images per action differs from person to person.

3.2.5 Deep Learning Model for Activity Classification

A CNN model, illustrated in figure 3.17, was trained as a classifier of actions. It takes each activity image as an input and provides the prediction in the form of the probability distribution on the five actions. Values of each activity image were normalized to be within the interval [0, 1] before being fed into the 3×3 convolutions of CNN architecture. After two convolutions, a max-pooling operation with a 2×2 filter down-sampled the dimension of the feature map into half of the input size. Then again after two consecutive convolutions, second max-pooling operation down-sampled the feature map into the size of 25×3×128. Afterwards, the feature map was flattened into a feature vector of 9600 elements, which was subsequently densified to 256 feature vectors with a fully connected layer. Another fully connected layer is

used to further densify the feature vectors to the dimension of 5, that is the number of classes. This 5-dimensional score vector S_j $(j = 1,2 \ldots\ldots,5)$ depicts the predicted classification probabilities using a softmax function as follows:

$$P(y = j) = \frac{exp(S_j)}{\sum_{k=1}^{5} exp(S_k)} \ . \tag{3.2}$$

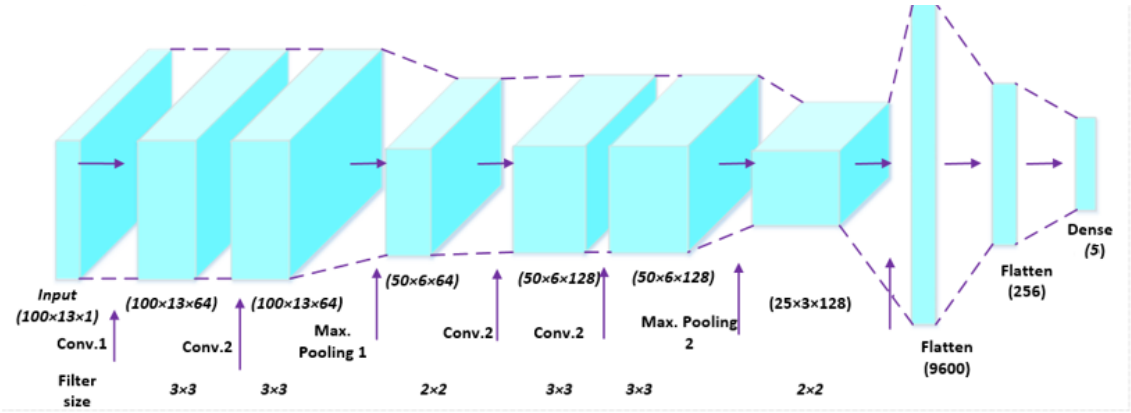

Figure 3.17 The CNN architecture for classification

Training a CNN model is basically about determining the optimal weights w for the network by minimizing a cost function. In this experiment the cost function is a categorical cross entropy. Dropout regularization was used to reduce the overfitting issue.

3.2.6 Evaluation of Experiment Results

3.2.6.1 Evaluation Methods

A commonly used evaluation metric, named accuracy, was used to evaluate the classification performance in this study. This metric is chosen because it is very intuitive, simple to understand, and easy to compute. Accuracy is computed as:

$$Accuracy = \frac{Number\ of\ correct\ predictions}{Total\ number\ of\ predictions} = \frac{TP+TN}{TP+TN+FP+FN}, \quad (3.2)$$

Where, TP, TN, FP, and FN stand for True Positive, True Negative, False Positive, and False Negative, respectively.

Two validation methods were used in this study: the train-test split (TTS) and Leave-One-Out (LOO), as figure 3.18 illustrates. The TTS evaluation used 80% data of every individual action of the four subjects as the training dataset and the remaining 20% data as the testing dataset. The classifier was trained using the training dataset, and its accuracy was measured on the test dataset. In TTS the data of each subject was present in both training and testing; therefore, the classifier learned the discriminative features of all subjects during the training. That is, the TTS evaluation method is to determine the performance of a trained model on the new data of the same group of subjects. The LOO evaluation used the data of three subjects as the training dataset, leaving out one subject for testing. The LOO evaluation method is to determine the performance of a trained model on new subjects. The LOO evaluation was repeated five times and each time a different subject was tested. The average performance on the five repetitions was used as the performance measurement of the classifier.

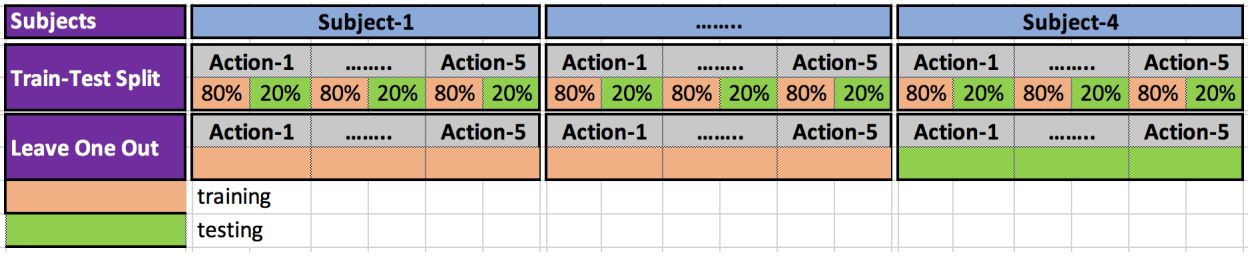

Figure 3.18 Illustration of TTS and LOO validation methods

3.2.6.2 Implementation of Fusion Method

As figure 3.12 shows, all five actions are involved with both hands, which indicates that both sources of data contain valuable information for providing discriminative features for action classification. Therefore, these two sources of data were combined and hopefully the fusion method would yield better classification results. The fusion strategy is illustrated briefly in figure 3.19.

Data Type	Architecture	Prediction Probabilities for 5 Actions					Predicted Action
		Action-1	Action-2	Action-3	Action-4	Action-5	
Right Hand(RH) IMU data	CNN Model	0.6	0.1	0.1	0.06	0.06	Action-1
Left Hand(LH) IMU data	CNN Model	0.2	0.4	0.15	0.08	0.06	Action-2
	Average Fusion	0.4	0.25	0.125	0.07	0.06	Action-1

Figure 3.19 Illustration of average fusion method

Two identical CNN models are trained on two sources of data – RH-IUM is the model trained on the right hand IMU data and LH-IMU is the one trained on the left hand IMU data. For every activity image, each of the two models provides its own prediction result in the format of a probability distribution on the 5 actions, as figure 3.19 shows. For example, the RH-IMU model predicts that the action is action-1 with a probability 0.6 and so on. The two models provide two different predictions. The average of the two probability distributions gives the final prediction.

3.2.6.3 Comparison of Model Performance using the TTS Validation Method

The 80% train -20% test TTS method was repeated for five times. In each run of the test, 20% of data were randomly sampled and used as the test dataset. The average of the five results

serves as an estimate of the classification accuracy. From figure 3.20 (a) it can be seen that the fusion method provides a little better accuracy than the other two models, but not at statistical significance. We further compared the three models as the action level, shown in figure 3.20 (b). When the performance difference between the LH-IMU and RH-IMU models is small, fusion method performs better (e.g., in recognition of action-3 & action-4 in this experimental study). If the difference between the LH-IMU and RH-IMU models is large, the fusion model may not perform better than every individual model (e.g., in recognition of action-1, -2, and -5 in this experimental study).

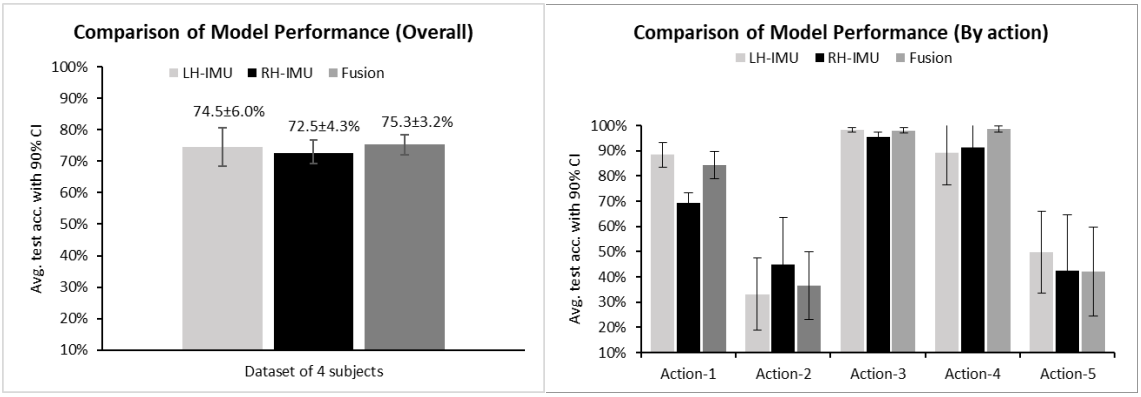

(a) (b)

Figure 3.20 Model performance comparison (a), the comparison at action level (b)

To learn details of misclassification, recognition accuracy (recall) and precision were calculated, displayed in figure 3.21. In both matrices the rows represent the ground truth actions and the columns represent the predicted actions. The diagonal elements count the correct classifications. From both matrices we can see that, the performances of action recognition on action-1, action-3, and action-4 were satisfactory. Most misclassifications occurred between

action-2 and action-5. The reason for the misclassification is action-2 (loading into trolley) and action-5 (unloading from trolley) are similar with each other.

	Action-1	Action-2	Action-3	Action-4	Action-5
Action-1	84.83%	7.30%	1.12%	2.25%	4.49%
Action-2	2.73%	44.09%	5.91%	10.00%	37.27%
Action-3	0.61%	1.23%	97.85%	0.00%	0.31%
Action-4	0.00%	1.85%	0.00%	98.15%	0.00%
Action-5	2.73%	44.09%	5.91%	10.00%	37.27%

(a)

	Action-1	Action-2	Action-3	Action-4	Action-5
Action-1	91.52%	6.02%	0.58%	1.28%	4.62%
Action-2	3.64%	44.91%	3.75%	7.03%	47.40%
Action-3	1.21%	1.85%	91.93%	0.00%	0.58%
Action-4	0.00%	2.31%	0.00%	84.66%	0.00%
Action-5	3.64%	44.91%	3.75%	7.03%	47.40%

(b)

Figure 3.21 Recognition accuracy (recall) (a), precision (b)

3.2.3.4 Comparison of Model Performance using the LOO Validation Method

We also evaluated the three models using the LOO method. The performance of any model evaluated using the LOO method is lower than that evaluated using the TTS method, as figure 3.22 shows. This is due to the fact that the testing dataset in LOO method is from a new subject who has unique behavior not appeared in the training dataset. Figure 3.22 further shows that the performances of the fusion model evaluated using the two methods are close to each other, indicating that fusion is helpful when a trained model is used to recognize activities of new subjects.

We further compared the performances of the three models at the subject level and action level. At the subject level, the fusion model outperformed the RH-IMU model and the LH-IMU model for recognizing actions of each subject. At the action level, the fusion model is better than

the other two models in recognizing actions 1, 3, and 4. When recognizing actions 2 and 5, the two actions with relatively higher degree of confusion, the fusion model had similar performance as the RH-IMU model.

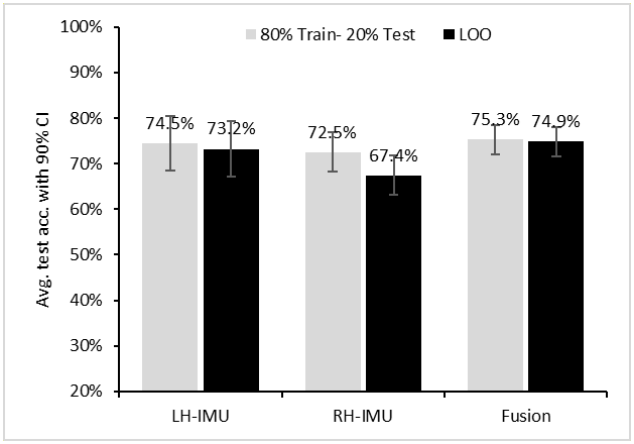

Figure 3.22 Comparison between two validation methods

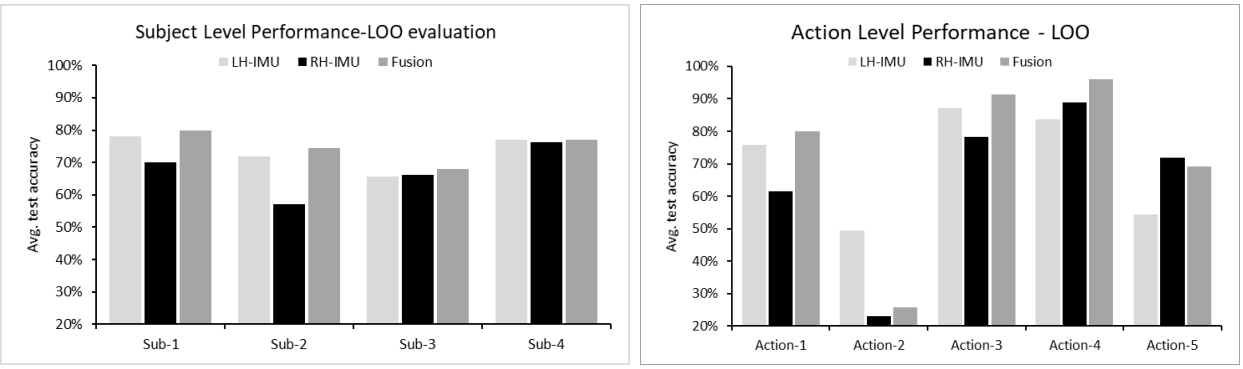

(a) (b)

Figure 3.23 Comparison of model performance evaluated using the LOO evaluation: subject level (a), action level (b)

3.2.7 Conclusion

In this study we used Myo armbands to collect the IMU data of workers and developed two CNN models, the RH-IMU model and LH-IMU model, to recognize worker actions in the loading and unloading operations. The dataset we obtained for this study contains five actions of four subjects in ten repetitions. Model fusion was further applied to improve the performance of the CNN models. The use of model fusion yields the third CNN model of this study. Both the TTS method and the LOO method were used to evaluate the performance of the three models. Although both LH-IMU and RH-IMU models are found to be less capable in the LOO evaluation than in the train-test split evaluation, model fusion can help improve the ability to recognize actions of new subjects. Challenges are present in recognizing actions with similarity.

In this study only the IMU data were used for action recognition. An immediate extension of the current work is to add the EMG data to improve the ability of action recognition. In the LOO evaluation, low performance was observed in correctly recognizing actions with similarity. Fine tuning the model using a small amount of data of new subjects would help improve the model performance in recognizing the actions of new subjects.

Chapter 4 Feedback Systems for Enhancing Risk Awareness: System Design and Prototyping

4.1 Introduction

The rapid development of sensing, communication, and cloud computing technologies has promoted the growth of connected smart systems for various applications. This chapter presents a study of developing feedback systems for enhancing the risk awareness of workers. Two prototype systems that use different technologies were developed and evaluated in this project. Both systems trigger the feedback to a worker according to define distances of the worker from the hazardous material (hazmat). The systems can be easily modified to adapt to other mechanisms of triggering the feedback.

4.2 The BLE Based System

4.2.1 System Design

The Bluetooth Low Energy (BLE) based system, illustrated in figure 4.1, is composed of three components: a BLE based proximity sensor, safety information, and a mobile device being used by the worker which can receive the information. The sensor is physically attached to or within a short range of the hazardous material. The safety information is then either presented as a local notification or a webpage. The sensor attached to the hazardous material is associated with the safety information of the material through the cloud management system of the sensor. When a worker with an associated mobile device enters the defined broadcast range of the proximity sensor, the sensor detects the worker and pushes the safety information to the receiving device. By reviewing the provided information, the worker's awareness is reinforced of the presence of the hazardous material, potential risks of transporting the material, and safety guidelines related to the material in question.

Figure 4.1 Schematic diagram of the BLE based feedback system

4.2.2 System Prototyping

4.2.2.1 Safety Information

The safety information about a hazmat may include the description of the hazmat, personal protection equipment (PPE) required, and safety operation guidance. In this project we have two versions of safety information: detailed information and brief information.

Detailed safety information. We presented the detailed information of each class of hazmat in a webpage illustrated in figure 4.1 (a). The webpage for each class of hazmat mainly includes the following three sections:

- Key Alarm Message: a brief statement and a standard dangerous product classification icon to prompt workers approaching this area.
- Check List of Required PPE: according to the category of hazmat stored in the area, required PPE and corresponding icons are listed so that the workers can check by themselves if all required PPE have been worn appropriately.

- Information on the Specific Class: the hazmat class definition, subcategories of hazmat within the class, and commonly transported hazmat in this class.

A link to section three was embedded in the statement of section one in the webpage. Those who come in contact with the area on a normal basis should be familiar with the nature of the hazmat they are approaching, so there is not as great of a need to see section three. However, workers who are not familiar with, or cannot recognize, the nature of the hazmat in question are able to jump to this section quickly through the provided link in the first section.

The Uniform Resource Locator (URL) of a webpage is the reference address that identifies where the webpage is located on the internet. The URL is a vital part of the feedback system since it provides access to the webpage intended to be displayed to the worker. The URL is pushed to the receiving device of the worker through a mobile app. Figure 4.2(b) displays the notification generated by a mobile app we developed for this project and figure 4.2(c) is the nearby notification generated by Physical Web, an app provided by Google.

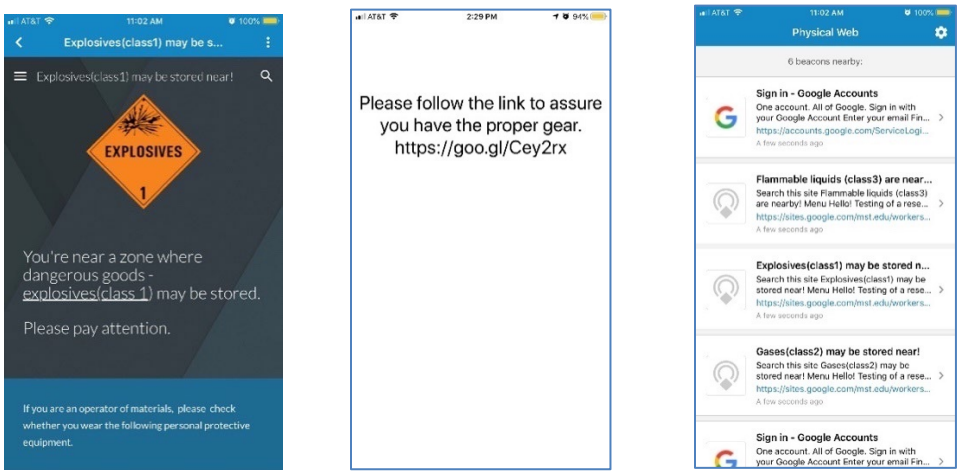

(a) (b) (c)

Figure 4.2 Safty information webpage (a), local notifiation (b), Physical Web notification (c)

Brief safety information. If workers choose to not click the link to the webpage, they will not view the safety information in the webpage. Therefore, the other approach is to directly present brief safety information as notifications of a mobile app and push the notifications to the receiving devices of workers. Figure 4.3 illustrates three short notifications displayed by the mobile app in the receiving device.

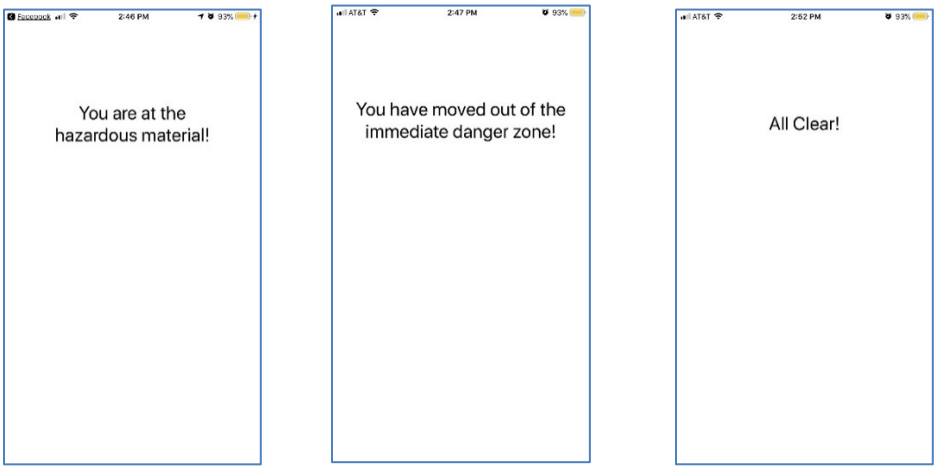

(a) (b) (c)

Figure 4.3 Notifications: when entering the inner zone of hazmat (a), when leaving the inner zone of hazmat (b), and when leaving the outer zone (c)

4.2.2.2 Proximity Sensor

We chose BLE proximity beacons produced by Estimote®. A beacon is a tiny device that broadcasts Bluetooth data packets understood by compatible receiving devices. The data packets are random sets of letters and digits, which contain the unique identity of the beacon and other data. The exact look of those packets and their capabilities are determined by certain protocols such as Eddystone, Estimote Monitoring, or iBeacon. Almost every iOS and Android Bluetooth-enabled device is compatible with each of these protocols.

Beacons broadcast them with a certain strength in all possible directions. Therefore, we can select and define distances for receiving specific data packets. For example, when a worker with a mobile device enters a zone defined by a distance we select, a corresponding beacon packet is sent to the designated mobile app installed in the receiving device. When the packet arrives, the app is immediately launched and it asks the Estimote Cloud for the instruction on what to do about this particular beacon. The Cloud, in milliseconds, returns the necessary information and the app performs the programmed activity, which in this app is to display a notification.

We can manage settings of beacons in Estimote Cloud displayed in figure 4.4, which includes, but is not limited to, monitoring the beacon's battery power, transmitting power, and location. In addition, the time stamp of when workers are near the beacon can be recorded and a statistical graph can be automatically generated.

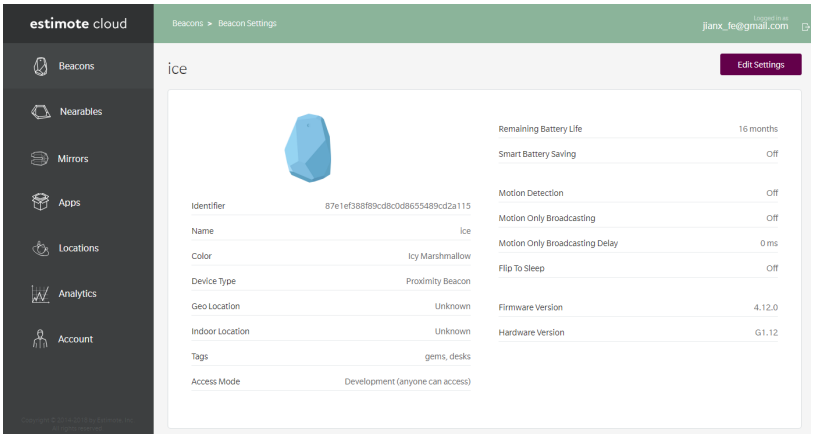

Figure 4.4 Screenshot of the Estimote Cloud

4.2.2.3 Mobile Applications

A beacon needs to be connected to a mobile app that performs designed activities to

interact with workers. We can either build our own ISO/Android app or use one of the available third-party apps. In this project we used Physical Web provided by Google and also developed our own ISO app.

Physical Web. It is a mobile app which can receive URL messages sent by beacons. For Android devices, the app needs to be downloaded from Google Play. When the screen is locked, the user receives a push message and is able to quickly reach to the webpage to review the provided information. At the same time, Android users who do not install the application can receive URL push messages by opening the Bluetooth and location functions. For Apple devices, it is necessary to download the application through Apple's App Store, as an installed app is the only way one can access the URL information from the beacon. In addition, Physical Web has the ability to not only find the signal from the beacon, but also the BLE signals of all nearby devices, such as the Bluetooth signal of a printer. If there were not a large number of other devices in the application environment, this situation did not have a substantial impact on the beacon users.

Self-developed App. As a further measure of testing the proximity beacons, we developed an app that can display various notifications (see fig. 4.3) depending on where the worker is. The app defines an inner zone and an outer zone of the hazmat: the average radius of the inner zone and outer zone are 1.5 meters and 5 meters, respectively. Designers can customize the number of zones and their ranges based on specific needs of implementation. When the worker enters or leaves a zone, a corresponding notification is displayed on the interface of the app. This app was then further updated to display the URL as well, as figure 4.2 (b) illustrates, similar to what the Physical Web application provides.

4.3 Arduino Based System

4.3.1 System Design

The second prototype system, as illustrated in figure 4.5, is composed of an Arduino development board, a ranging sensor, and one or multiple feedback devices. The ranging sensor is attached to the Arduino board and the board is with the hazmat. Brief safety information of the hazmat has been saved in the board. When a worker enters a zone near the hazmat, which is defined by specifying the detectable range of the ranging sensor, either the safety information is displayed in a displaying device or an alarm is provided by the buzzer.

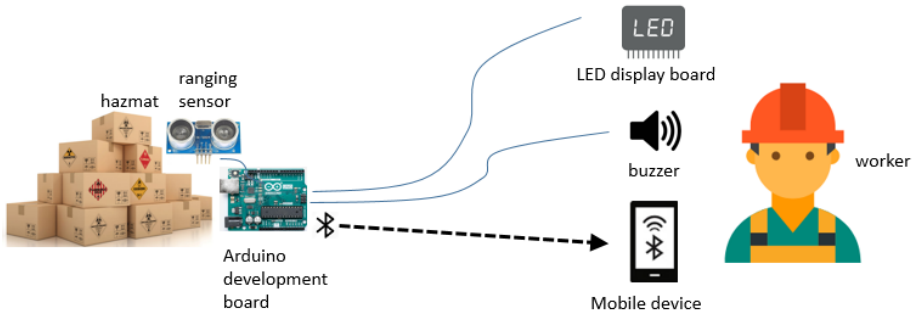

Figure 4.5 Schematic diagram of the Arduino based feedback system

4.3.2 System Prototyping

The prototype of the Arduino based system is displayed in figure 4.6.

4.3.2.1 Ranging Sensor

We chose the Ultrasonic sensor HC SR 04 that provides from 2 cm to 400 cm non-contact measurement function. The measurement precision is up to 0.3cm.

4.3.2.2 Receiving devices

Receiving devices are used for either visually displaying safety information or broadcasting an alarming sound to workers. This project tested three types of receiving devices: a buzzer, a light emitting diode (LED) screen, and a smart mobile phone. A Bluetooth HC 05

unit was used for transmitting the safety information to the mobile phone of the worker. As figure 4.5 shows, the buzzer, LED screen, and the Bluetooth unit are connected to the Arduino board using wires.

4.3.2.3 Arduino Uno Board

Arduino Uno is the best board to get started with electronics and code the output displayed on receiving devices. We used the open-source Arduino software (IDE) to write code and upload it to the board. The language we used to compile the code is C. First, the board is programmed to be able to trigger the buzzer, display a message on the LED screen, or transmit the message to the mobile phone through the Bluetooth unit when the worker enters a pre-specified detectable range of the ranging sensor. There are three major things that need to be specified in programming: (1) define the pin, (2) set up the input and output, and (3) write the function of the program. For example, the input is the distance measurement of the ultrasonic ranging sensor, the output is a message “in the range of hazmat class 1” to be displayed on the LED screen, and the function is to trigger the output when a worker enters the detectable range of the ranging sensor.

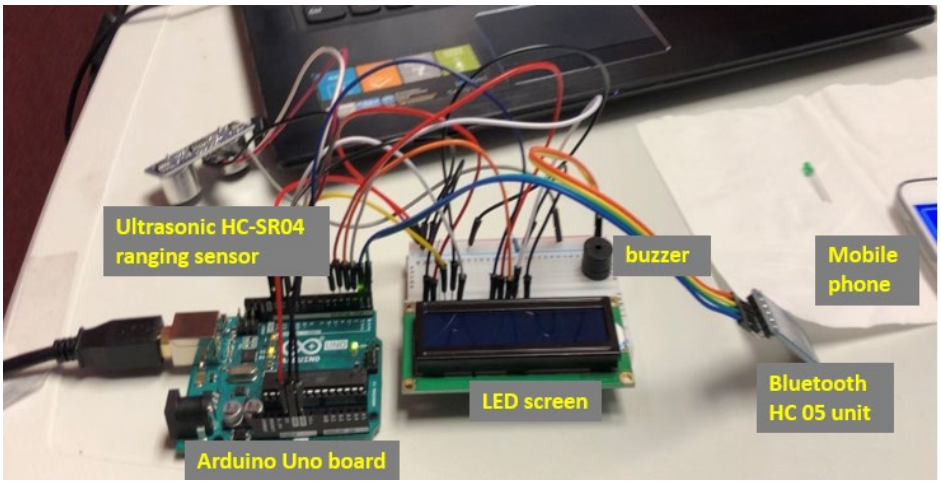

Figure 4.6 The prototype of Arduino based system

Then, the board is connected to the computer to get the complied program uploaded. When uploading the program, it is important to disconnect the Bluetooth unit from the board before uploading the program. After the program is uploaded successfully, the Bluetooth module is reconnected to the board. Otherwise, program uploading would fail.

4.4 Comparison

The following is the comparison of the two systems in terms of the technologies they use, which is also summarized in table 4.1.

- BLE beacon has considerable reduced power consumption and, therefore, it can be widely deployed. The ultrasonic ranging sensor requires stable power supply and consumes more power than BLE. But the measurement precision of ultrasonic ranging sensor is much higher than BLE beacon.
- Smart mobile devices are able to display detailed information and can interact with users. The use of smart mobile devices as receiving devices requires Bluetooth wireless communication. The buzzer and LED screen can deliver only simple information and, thus, they are usually set up as stationary devices connected to power sources.
- The BLE based system stores most data such as beacon information, safety information, beacon functions, and commands in the cloud. The Arduino based system stores most information in the board. The cloud is much more capable than the board in terms of information storage and processing, computation, analytics, and so on.
- Codes for the BLE based system was developed using Xcode in this project and codes for the Arduino based system was developed using C. Both system requires the

efforts of programming.

Table 4.1 Comparison of the systems by technologies

	BLE based System	**Arduino based System**
Sensor	BLE Estimote proximity beacon	Ultrasonic ranging sensor HC-SR04
Communication	Bluetooth wireless communication	Wire communication mainly, Bluetooth can be used
Receiving devices	Smart phone	Buzzer, LED screen, smart phone
Information Storage, processing and so on	Beacon Cloud	Arduino board
Development environment	Xcode	Arduino IDE

4.4 Conclusions

This chapter presented a study of designing and prototyping two feedback systems for enhancing workers' awareness of risks when approaching hazmat. While each of the two prototype systems certainly provide the desired function of enhancing risk awareness to a certain extent, their strengths and limitations were mainly seen from the perspective of technologies they use. BLE beacons are powered by batteries and have very low power consumption. Therefore, they can be widely deployed with minimal maintenance. The ultrasonic ranging sensor used in this study does not have this advantage. It is, however, more accurate than a BLE beacon in measuring distance. Cloud computing offers superior capabilities in storage, software, analytics, security, and extensible architecture allowing developers and clients alike to create functionality tailored to the system requirements at hand. The aforementioned set of features is not available when using the Arduino development board due to the limited capabilities of the platform. Smart devices carried by workers are mobile devices that can move with the workers, display rich

information to them if needed, and interact with them. Buzzers and LED boards can only provide simple feedback to workers, and lack mobility as they are connected to the Arduino board using wires.

The analysis of each system's strengths and limitations within this study suggest ways of improving the smart system design which include: augmenting the distance measurement accuracy of BLE beacons, improving the modularity of the simple feedback devices, and protecting the privacy of each worker's smart mobile device(s) while collecting data to utilize the system.

Chapter 5 Conclusions and Future Work

5.1 Conclusions

Results and findings from this project allow for drawing the following conclusions and recommendations on developing assistance systems for enhancing the safety of transportation workers.

5.1.1 System Architecting

In this project we architected a system for assisting hazmat transportation workers as a CPS. Transportation workers and their workplace form the physical system that we would like to understand, analyze, and assist. We created the "digital twin" of the physical system using methods of system analytics, including descriptive data analysis, predictive machine learning, and decision analysis. The physical system and its digital twin are seamlessly synergized as a CPS through sensing, communication, and feedback technologies. Results of this project demonstrate that architecting the smart assistance system as a CPS is appropriate in that the desired capabilities are obtained, including the real-time understanding, reasoning, and learning of transportation workers and their workplace, as well as the optimization of the intervention and assistance to workers.

5.1.2 System Analytics

From this project we found that an important driver of smartness is the digit twin of the physical system. The quality of the digit twin determines how much we can help the physical system. We implemented analytic methods, which are either fundamental or relatively mature, to quickly build the digital twin of the physical system that we would like to inference, analyze, and assist. Descriptive data analysis and a data unfolding strategy were used to identify high chance

scenarios of HMHIs. While these methods are fundamental, in this project they have been tested to be effective in delivering the needed information.

Activities of hazmat transportation workers have not been widely studied. Therefore, existing activity recognition models may not do a better job than NNs specifically trained using the data of hazmat transportation workers. We trained our own NNs on small datasets collected by the project, which recognize worker actions in their daily operations with reasonably good quality. Yet it is very reasonable to fine-tune existing NN models for classifying and recognizing elements in the workplace (vehicle, humans, tools, and equipment to name a few), because these elements are broadly present in many public large datasets used for training those existing models.

Providing workers assistance only when they need would maximize the effectiveness of the assistance system and minimize the distraction of them from unnecessary help. To serve this purpose, simple decision rules were tested in this project, which mainly use thresholds to control the trigger of assistance. These threshold based rules are verified to be effective and reliable.

5.1.3 Technology Architecture for System Integration

Seamlessly integrating the digital twin with the physical system to allow for real-time interaction and collaboration between them is the way of creating synergy. Results of this project confirm that sensing, communication, and feedback/control technologies play critical roles of system integration.

When prototyping the smart assistance system in this project, we made efforts to try and evaluate different options of sensing, communication and feedback technologies. For the purpose of rapid system prototyping, we chose hardware and parts that are commercially available and provide development functions. Sensors we used in this project include the Myo armband – a

wearable device providing IMU and EMG sensor data of workers, camera – vision based sensor mounted on vehicles or set up in the workplace to capture video data of workers and operation environments, and BLE Estimote beacon – providing proximity, temperature and accelerometer data of any elements attached with the beacon. We found that sensor fusion (i.e., combination of multiple sensors or sensor data models) is the way of creating comprehensive, reliable, and effective sensing capability.

We used both wire and wireless communication (Bluetooth) technology. Wireless communication has been justified to be a necessity for a smart assistance system due to the mobility requirement. Yet wire communication can be a complementary method due to the easy use and high reliability.

A range of feedback devices were tested: buzzers providing audio alarms, an LED screen that can show a short notification, apps installed in users' mobile devices which feed more details to users and have interactions with users, and websites that literally can display as much information as needed. The development effort on a feedback device/method is positively correlated with the volume of information to deliver and how smart it is in interacting with users.

The choices of sensing, communicating, and feedback technologies are not independent. A technology architecture composed of sensor fusion, wireless communication, cloud computing, and smart mobile devices is highly recommended based on results of this project.

5.2 Future Work

Completion of this project is not the end. Findings from the project and accumulated knowledge have built a foundation for expanding and continuing the current studies. In the following we summarize some future work identified as highly valuable.

5.2.1 Incident Classification using Descriptive Data Mining Methods

While the current project mainly uses descriptive analysis of incident data to identify scenarios of high chance HMHIs, we would recommend extending the current descriptive analysis of incident data to advanced descriptive data mining methods (such as clustering analysis and association rules) to be able to handle big incident data. We can classify incidents occurring in history according to incident consequences (No. fatalities, No. hospitalized injuries, financial damage, evacuation, and so on) and characteristics (rollover, hit, fire, and etc.) to identify and characterize incident clusters that require particular attention.

5.2.2 Enhanced Road Scene Analysis with Transfer Learning

The transportation phase with the largest number of HMHIs is "In Transit" and top causes of these incidents overlap with causes for other transportation incidents. Assistance to transportation workers when they are driving would produce great benefits. The method of road scene analysis presented in this project works under normal daylight driving conditions. However, false detections are commonly observed from experiments of driving conditions with low visibility such as night time or bad weather. To obtain reliable results of road scene analysis in various driving conditions, special sensors such as infrared cameras can be added. Moreover, NNs are fine-tuned with video data collected from conditions with low visibility. False detected images are annotated again and then used to improve the tool. We can improve the tool in an iterative manner until the percentage of false detection drops below the pre-defined threshold.

5.2.3 Incident Occurrence Prediction

Predicting the occurrence of incidents even just a couple of seconds ahead would allow for providing alarms or assistance to workers. Accurately triggering the assistance to workers is extremely important. We are motivated to further study a way of determining a more

informative, reliable threshold for triggering assistance. Predictive data mining methods (e.g., logistic regression classification, classification trees, k-nearest neighbors) can be used to create incident classifiers that each predicts the occurrence of any type of incident according to the assessment of pre-incident risk factors (e.g., road condition, road type, weather, to name a few).

References

Abkowitz, M, D., DeLorenzo, J. P., Duych, R., Greenberg, A., & McSweeney, T. (2001). Assessing the economic effect of incidents involving truck transport of hazardous materials. *Transportation Research Record*, 1763, 125-129.

Anguita, D., Ghio, A., Oneto, L., Parra, X., & Reyes-Ortiz, J. L. (2012, December). Human activity recognition on smartphones using a multiclass hardware-friendly support vector machine. In International workshop on ambient assisted living (pp. 216-223). Springer, Berlin, Heidelberg.

Bureau of Transportation Statistics. 2016 Transportation Statistics Annual Report. https://www.rita.dot.gov/bts/sites/rita.dot.gov.bts/files/publications/transportation_statistics_annual_report/2016/index.html. Accessed on June 25, 2017.

Bojarski, M., Del Testa, D., Dworakowski, D., Firner, B., Flepp, B., Goyal, P., & Zhang, X. (2016). End to end learning for self-driving cars. arXiv preprint arXiv:1604.07316.

Catal, C., Tufekci, S., Pirmit, E., & Kocabag, G. (2015). On the use of ensemble of classifiers for accelerometer-based activity recognition. Applied Soft Computing, 37, 1018-1022.

Clark, R. M., & Besterfield-Sacre, M. E. (2009). A new approach to hazardous materials transportation risk analysis: Decision modeling to identify critical variables. *Risk Analysis*, 29(3), 344-354.

Du, X., El-Khamy, M., Lee, J., & Davis, L. (2017, March). Fused DNN: A deep neural network fusion approach to fast and robust pedestrian detection. In Applications of Computer Vision (WACV), 2017 IEEE Winter Conference on (pp. 953-961). IEEE.

Electronic Code of Federal Regulations (ECFR). (2018). *Title 49 Transportation -171.15 Immediate Notice of Certain Hazardous Materials Incidents*. Retrieved from ECFR: https://www.ecfr.gov/cgi-bin/text-idx?SID=04597e55b2b1ab04e0b02b15ebb7e68f&mc=true&node=se49.2.171_115&rgn=div8

Federal Motor Carrier Safety Administration (FMCSA). (n.d.). *Federal Motor Carrier Safety Regulations – Section 390.5*. Retrieved from FMCSA: https://www.fmcsa.dot.gov/regulations/title49/section/390.5

Harwood, D. W., Russell, E. R., & Viner, J. G. (1989). Characteristics of accidents and incidents in highway transportation of hazardous materials. *Transportation Resaerch Record*, 1245, 23-33.

Hwang, S, Brown, D., O'Steen, J., Policastro, A., & Dunn, W. (2001). Risk assessment for national transportation of selected hazardous materials. *Transportation Research Record*, 1763, 114-124.

Ha, S., & Choi, S. (2016, July). Convolutional neural networks for human activity recognition using multiple accelerometer and gyroscope sensors. In Neural Networks (IJCNN), 2016 International Joint Conference on (pp. 381-388). IEEE.

Häne, C., Sattler, T., & Pollefeys, M. (2015, September). Obstacle detection for self-driving cars using only monocular cameras and wheel odometry. In Intelligent Robots and Systems (IROS), 2015 IEEE/RSJ International Conference on (pp. 5101-5108). IEEE.

He, K., Gkioxari, G., Dollár, P., & Girshick, R. (2017, October). Mask r-cnn. In Computer Vision (ICCV), 2017 IEEE International Conference on (pp. 2980-2988). IEEE.

Jiang, W., & Yin, Z. (2015, October). Human activity recognition using wearable sensors by deep convolutional neural networks. In Proceedings of the 23rd ACM international conference on Multimedia (pp. 1307-1310). ACM.

Khaitan SK, McCalley JD (2015). Design techniques and applications of cyberphysical systems: A survey. *IEEE Systems Journal* 9(2): 350-65.

Lara, O. D., & Labrador, M. A. (2013). A survey on human activity recognition using wearable sensors. *IEEE Communications Surveys and Tutorials*, *15*(3), 1192-1209.

Lin, T. Y., Maire, M., Belongie, S., Hays, J., Perona, P., Ramanan, D. & Zitnick, C. L. (2014, September). Microsoft coco: Common objects in context. In European conference on computer vision (pp. 740-755). Springer, Cham.

Nath, N. D., Shrestha, P., & Behzadan, A. H. (2017, December). Human activity recognition and mobile sensing for construction simulation. In Simulation Conference (WSC), 2017 Winter (pp. 2448-2459). IEEE.

Nweke, H. F., Teh, Y. W., Al-Garadi, M. A., & Alo, U. R. (2018). Deep learning algorithms for human activity recognition using mobile and wearable sensor networks: State of the art and research challenges. Expert Systems with Applications.

Occupational Safety and Health Administration (OSHA). (n.d.). *Hazardous Material Transportation Act of 1975*. Retrieved from US Department of Labor: https://www.osha.gov/SLTC/trucking_industry/transportinghazardousmaterials.html

Office of Hazardous Materials Safety (2017). US Department of Transportation Pipeline and Hazardous Materials Safety Administration. *Top consequence hazardous materials by commodities & failure modes, 2010-2014*.

Office of Hazardous Materials Safety (2011). US Department of Transportation Pipeline and Hazardous Materials Safety Administration. *Top consequence hazardous materials by commodities & failure modes, 2005-2009*.

Pipeline and Hazardous Materials Safety Administration (PHMSA). (n.d.). *Incident Report Data*. Retrieved from PHMSA Incident Report Database: https://hazmatonline.phmsa.dot.gov/IncidentReportsSearch/Welcome.aspx

Raso, R., Emrich, A., Burghardt, T., Schlenker, M., Gudehus, T., Sträter, O., & Loos, P. (2018). Activity monitoring using wearable sensors in manual production processes-an application of CPS for automated ergonomic assessments.

Shoaib, M., Bosch, S., Incel, O., Scholten, H., & Havinga, P. (2015). A survey of online activity recognition using mobile phones. Sensors, 15(1), 2059-2085.

Song, H., Choi, I. K., Ko, M. S., Bae, J., Kwak, S., & Yoo, J. (2018, January). Vulnerable Pedestrian detection and tracking using deep learning. In Electronics, Information, and Communication (ICEIC), 2018 International Conference on (pp. 1-2). IEEE.

Tefft, B. C. (2016). The Prevalence of Motor Vehicle Crashes Involving Road Debris, United States, 2011-2014. Age (years), 20(5.7), 10-1.

Tian, Y., Luo, P., Wang, X., & Tang, X. (2015). Pedestrian detection aided by deep learning semantic tasks. In Proceedings of the IEEE Conference on Computer Vision and Pattern Recognition (pp. 5079-5087).

United Nations, Department of Economic and Social Affairs, (2018). "68% of the world population projected to live in urban areas by 2050, says UN". Available at https://www.un.org/development/desa/en/news/population/2018-revision-of-world-urbanization-prospects.html

US Department of Transportation Pipeline and Hazardous Materials Safety Administration (PHMSA). *Hazmat transportation training requirements*. *An overview of 49 CFR parts 172-173*.

US Department of Transportation. *Beyond traffic 2045: Trend and choices*. 2015.

US Department of Transportation Pipeline and Hazardous Materials Safety Administration (PHMSA). *Incident Statistics*.https://www.phmsa.dot.gov/hazmat/library/data-stats/incidents. Accessed on June 25, 2017.

US Department of Transportation Federal Highway Administration (FHWA). Work Zone Management Program. https://ops.fhwa.dot.gov/wz/workersafety/#wv. Accessed on June 25, 2017.

Xu, D., Ouyang, W., Ricci, E., Wang, X., & Sebe, N. (2017, July). Learning cross-modal

deep representations for robust pedestrian detection. In Proc. of the IEEE Conf. on Computer Vision and Pattern Recognition (CVPR).

Zeng, M., Nguyen, L. T., Yu, B., Mengshoel, O. J., Zhu, J., Wu, P., & Zhang, J. (2014, November). Convolutional neural networks for human activity recognition using mobile sensors. In Mobile Computing, Applications and Services (MobiCASE), 2014 6th International Conference on (pp. 197-205). IEEE.

Zhang, M., & Sawchuk, A. A. (2013). Human daily activity recognition with sparse representation using wearable sensors. IEEE journal of Biomedical and Health Informatics, 17(3), 553-560.

Zhao, L, Wang, X., & Qian, Y. (2012). Analysis of factors that influence hazardous material transportation accidents based on Bayesian networks: A case study in China. *Safety Science*, 50(4), 1049-1055.